TITLE: Sex differences in islet stress responses support female beta cell resilience

SHORT TITLE: Sex-specific beta cell stress responses

AUTHORS: George P. Brownrigg[1], Yi Han Xia[1], Chieh Min Jamie Chu[1], Su Wang[1], Charlotte Chao[1], Jiashuo Aaron Zhang[1], Søs Skovsø[1], Evgeniy Panzhinskiy[1], Xiaoke Hu[1], James D. Johnson[1§], Elizabeth J. Rideout[1§]

AFFILIATION: [1]Department of Cellular and Physiological Sciences, Life Sciences Institute, The University of British Columbia, 2350 Health Sciences Mall, Vancouver, BC, V6T 1Z3, Canada

§ CO-CORRESPONDING AUTHORS: Department of Cellular and Physiological Sciences, Life Sciences Institute, The University of British Columbia, 2350 Health Sciences Mall, Vancouver, BC, V6T 1Z3, Canada. Email: elizabeth.rideout@ubc.ca & james.d.johnson@ubc.ca Phone: (604) 822-0623 & (604) 822-7187. Fax: (604) 822-2316.

AUTHOR CONTRIBUTIONS

G. P. B. conceived studies, conducted experiments, interpreted experiments, wrote the manuscript
Y. X. performed bioinformatic analysis and data visualization
J. C. created custom R scripts (single-cell GFP tracking)
S. W. analyzed data (human RNAseq)
C. C. created custom R scripts (mouse RNAseq analysis)
J. A. Z. analyzed data (HPAP perifusions)
S. S. conducted experiments (*in vivo* physiology)
E. P. conducted experiments (islet western blots)
X. H. conducted experiments (dissections)
J. D. J. conceived studies, interpreted experiments, edited the manuscript
E. J. R. conceived studies, interpreted experiments, edited the manuscript, and is the guarantor of this work

KEYWORDS: pancreatic islets, β cells, diabetes mellitus, endoplasmic reticulum stress, protein synthesis, transcriptomics

ABSTRACT

Objective: Pancreatic β cells play a key role in glucose homeostasis; dysfunction of this critical cell type causes type 2 diabetes (T2D). Emerging evidence points to sex differences in β cells, but few studies have examined male-female differences in β cell stress responses and resilience across multiple contexts, including diabetes. Here, we address the need for high-quality information on sex differences in β cell/islet gene expression and function using both human and rodent samples.

Methods: We compared β cell gene expression and insulin secretion in donors living with T2D to non-diabetic donors in both males and females. In mice, we generated a well-powered islet RNAseq dataset from 20-week-old male and female siblings with equivalent insulin sensitivity. Because on our unbiased analysis of gene expression pointed to sex differences in endoplasmic reticulum (ER) stress response, we subjected islets isolated from age-matched male and female mice to thapsigargin treatment and monitored protein synthesis, cell death, and β cell insulin production and secretion. Transcriptomic and proteomic analyses were used to characterize sex differences in islet responses to ER stress.

Results: Our single-cell analysis of human β cells revealed sex-specific changes to gene expression and function in T2D, correlating with more robust insulin secretion in islets isolated from female donors living with T2D compared to male T2D donors. In mice, RNA sequencing revealed differential enrichment of unfolded protein response pathway-associated genes, where female islets showed higher expression of genes linked with protein synthesis, folding, and processing. This differential expression was biologically significant, as female islets were more resilient to ER stress induction with thapsigargin. Specifically, female islets maintained better insulin secretion and showed a distinct transcriptional response under ER stress compared with males.

Conclusions: Our data demonstrate that physiologically significant sex differences in β cell gene expression exist in both humans and mice, and that female β cells maintain better insulin production and secretion across multiple physiological and pathological contexts.

1. Introduction

Pancreatic β cells make and secrete insulin, an essential hormone required to maintain whole-body glucose homeostasis. Emerging evidence from multiple species suggests biological sex is an important, but often overlooked, factor that affects β cell biology (1–6). Large-scale surveys of gene expression in mice and humans show that differences exist between the sexes in the pancreas (7–9), in islets (10), and in β cells specifically (4,11). Humans also have a sex-specific β cell gene expression response to aging (12), and show male-female differences in pancreatic β cell number (6). With respect to β cell function, most data from rodent and human studies suggests glucose-stimulated insulin secretion is higher in females than in males (5,10,13–16). While male-female differences in peripheral insulin sensitivity (15,17–27) may contribute to these differences, sex-biased insulin secretion in humans persists in the context of equivalent insulin sensitivity between males and females (5). Whether sex differences in additional aspects of β cell gene expression and function similarly persist remains unclear, as insulin sensitivity is not routinely monitored across datasets showing sex differences in β cell biology.

Biological sex also affects the risk of developing T2D. Across many population groups, men are at a higher risk of developing T2D than women (28–31). Some of the differential risk is explained by lifestyle and cultural factors (31–33). Biological sex also plays a role, however, as the male-biased risk of developing diabetes-like phenotypes exists across multiple animal models (22,34–39). Despite a dominant role for β cell function in T2D pathogenesis (40,41), T2D- and stress-associated changes to β cell gene expression and function in each sex remain largely unexplored, as many studies on this topic did not include biological sex as a variable in their analysis (42–49). More detailed knowledge of β cell gene expression and function in physiological and pathological contexts is therefore a key first step toward understanding how sex differences in this important cell type may contribute to T2D risk.

The overall goal of our study was to provide detailed knowledge of β cell gene expression and function in both males and females across multiple contexts to advance our understanding of sex differences in this important cell type. Collectively, our data show significant sex differences in islet and β cell gene expression and stress responses in both humans and mice. These differences contribute to sex differences in β cell resilience, where we find female β cells maintain better insulin secretion in response to stress and T2D. Importantly, these differences cannot be fully explained by differential peripheral insulin

99 sensitivity between the sexes, suggesting biological sex is an important variable to consider in
100 studies on islet and β cell function.
101
102 **2. Materials and methods**
103 ***2.1. Animals***
104 Mice were bred in-house or purchased from the Jackson Laboratory. Unless otherwise stated
105 mouse islets were isolated from C57BL/6J mice aged 20-24 weeks. Animals were housed
106 and studied in the UBC Modified Barrier Facility using protocols approved by the UBC Animal
107 Care Committee and in accordance with international guidelines. Mice were housed on a 12-
108 hour light/dark cycle with food and drinking water *ad libitum*. Mice were fed a regular chow
109 diet (LabDiet #5053); 24.5% energy from protein, 13.1% energy from fat, and 62.4% energy
110 from carbohydrates.
111
112 ***2.2. Islet Isolation, Culture, Dispersion and Treatment***
113 Mouse islet isolations were performed by ductal collagenase injection followed by filtration
114 and hand-picking, using modifications of the protocol described by Salvalaggio (50). Islets
115 recovered overnight, in islet culture media (RPMI media with 11.1 mM D-glucose
116 supplemented with 10% vol/vol fetal bovine serum (FBS) (Thermo: 12483020) and 1% vol/vol
117 Penicillin-Streptomycin (P/S) (GIBCO: 15140-148)) at 37°C with 5% CO_2. After four washes
118 with Minimal Essential Medium [L-glutamine, calcium and magnesium free] (Corning: 15-015
119 CV) islets were dispersed with 0.01% trypsin and resuspended in islet culture media. Cell
120 seedings were done as per the experimental procedure (protein synthesis: 20,000 cells per
121 well, live cell imaging: 5,000 cells per well). ER stress was induced by treating islets with the
122 SERCA inhibitor thapsigargin. For assays less than 24 hours, we used (11.1 mM D-glucose
123 RPMI, 1% vol/vol P/S). For assays greater than 24 hours we used (11.1 mM D-glucose RPMI,
124 1% vol/vol P/S, 10% vol/vol FBS).
125
126 ***2.3. Analysis of protein synthesis***
127 Dispersed islets were seeded into an optical 96-well plate (Perkin Elmer) at a density of
128 approximately 20,000 cells per well islet culture media (11.1 mM D-glucose RPMI, 1% vol/vol
129 P/S, 10% vol/vol FBS). 24 hours after seeding, treatments were applied in fresh islet culture
130 media (11.1 mM D-glucose RPMI, 1% vol/vol P/S). After incubation, fresh culture media was
131 applied (11.1 mM D-glucose RPMI, 1% vol/vol P/S), supplemented with 20 μM OPP

132 (Invitrogen) and respective drug treatments. The assay was performed according to
133 manufacturer's instructions; cells were then imaged at 10x with an ImageXpress^{MICRO} high-
134 content imager and analyzed with MetaXpress (Molecular Devices) to quantify the integrated
135 staining intensity of OPP-Alexa Fluor 594 in cells identified by NuclearMask Blue Stain.
136
137 ***2.4. Live cell imaging***
138 Dispersed islets were seeded into 384-well plates (Perkin Elmer) at a density of
139 approximately 5,000 cells per well and allowed to adhere for 48 hours in islet culture media
140 (11.1 mM D-glucose RPMI, 1% vol/vol P/S, 10% vol/vol FBS). Cells were stained with
141 Hoechst 33342 (Sigma-Aldrich) (0.05 µg/mL) and propidium iodide (Sigma-Aldrich) (0.5
142 µg/mL) for one hour in islet culture media (11.1 mM D-glucose RPMI, 1% vol/vol P/S, 10%
143 vol/vol FBS) prior to the addition of treatments and imaging. 384-well plates were placed into
144 environmentally controlled (37°C, 5% CO2) ImageXpress^{MICRO} high content imaging system.
145 To measure cell death, islet cells were imaged every 2 hours for 84 hours, and MetaXpress
146 software was used to quantify cell death, defined as the number of Propidium Iodide-
147 positive/Hoechst 33342-positive cells. To measure *Ins2* gene activity, dispersed islets from
148 *Ins2*$^{GFP/WT}$ mice aged 21-23 weeks were used (51). Islet cells were imaged every 30 minutes
149 for 60 hours. MetaXpress analysis software and custom R scripts were used to perform
150 single-cell tracking of *Ins2*$^{GFP/WT}$ β cells as previously described (51).
151
152 ***2.5. Western blot***
153 After a 24-hour treatment with 1 µM Tg in islet culture media (11.1 mM D-glucose RPMI, 1%
154 vol/vol P/S, 10% vol/vol FBS), mouse islets were sonicated in RIPA lysis buffer (150 mM
155 NaCl, 1% Nonidet P-40, 0.5% DOC, 0.1% SDS, 50 mM Tris (pH 7.4), 2 mM EGTA, 2 mM
156 Na_3VO_4, and 2 mM NaF supplemented with complete mini protease inhibitor cocktail (Roche,
157 Laval, QC)). Protein lysates were incubated in Laemmli loading buffer (Thermo, J61337AC) at
158 95°C for 5 minutes and resolved by SDS-PAGE. Proteins were then transferred to PVDF
159 membranes (BioRad, CA) and probed with antibodies against HSPA5 (1:1000, Cat. #3183,
160 Cell Signalling), eIF2α (1:1000, Cat. #2103, Cell Signalling), phospho-eIF2α (1:1000, Cat.
161 #3398, Cell Signalling), IRE1α (1:1000, Cat. #3294, Cell Signalling), phospho-IRE1α (1:1000,
162 Cat. #PA1-16927, Thermo Fisher Scientific), CHOP (1:1000, #ab11419, Abcam), β-actin
163 (1:1000, NB600-501, Novus Biologicals). The signals were detected by secondary HRP-
164 conjugated antibodies (Anti-mouse, Cat. #7076; Anti-rabbit, Cat. #7074; CST) and either

165 Pierce ECL Western Blotting Substrate (Thermo Fisher Scientific) or Forte (Immobilon).
166 Protein band intensities were quantified using Image Studio (LI-COR).
167
168 ***2.6. Islet Secretion and Content***
169 Glucose-stimulated insulin/proinsulin production and secretion were assessed using size-
170 matched islets (five islets per well, in triplicate) seeded into 96-well V-bottom Tissue Culture
171 Treated Microplates (Corning: #CLS3894). Islets were allowed to adhere for 48 hours in
172 culture media (11.1 mM D-glucose RPMI, 1% vol/vol P/S, 10% vol/vol FBS). Islets were
173 washed with Krebs-Ringer Buffer (KRB; 129 mM NaCl, 4.8 mM KCl, 1.2 mM $MgSO_4$, 1.2 mM
174 KH_2PO_4, 2.5 mM $CaCl_2$, 5 mM $NaHCO_3$, 10 mM HEPES, 0.5% bovine serum albumin)
175 containing 3 mM glucose then pre-incubated for 4 hours in 3 mM glucose KRB. 1 μM Tg was
176 added to the 3 mM low glucose pre-incubation buffer 4 hours prior, 2 hours prior, or at the
177 start of the low glucose incubation period. Islets were incubated in KRB with 3 mM glucose
178 then 20 mM glucose for 45 minutes each. Supernatant was collected after each stimulation.
179 Islet insulin and proinsulin content was extracted by freeze-thawing in 100 μL of acid ethanol,
180 then the plates were shaken at 1200 rpm for 10 minutes at 4°C to lyse the islets. Insulin was
181 measured by Rodent Insulin Chemiluminescent ELISA (ALPCO: 80-INSMR) and proinsulin by
182 Rat/Mouse Proinsulin ELISA (Mercodia: 10-1232-01). Measurements were performed on a
183 Spark plate reader (TECAN).
184
185 ***2.7. Blood collection and in vivo analysis of glucose homeostasis and insulin secretion***
186 Mice were fasted for 6 hours prior to glucose and insulin tolerance tests. During glucose and
187 insulin tolerance tests, tail blood was collected for blood glucose measurements using a
188 glucometer (One Touch Ultra 2 Glucometer, Lifescan, Canada). For intraperitoneal (i.p.)
189 glucose tolerance tests, the glucose dose was 2 g glucose/kg of body mass. For insulin
190 tolerance tests, the insulin dose was 0.75U insulin/kg body mass. For measurements of *in*
191 *vivo* glucose-stimulated insulin secretion, femoral blood was collected after i.p. injection of 2 g
192 glucose/kg body mass. Blood samples were kept on ice during collection, centrifuged at 2000
193 rpm for 10 minutes at 4°C and stored as plasma at -20°C. Plasma samples were analysed for
194 insulin using Rodent Insulin Chemiluminescent ELISA (ALPCO: 80-INSMR).
195
196 ***2.8. RNA sequencing***

197 To assess basal transcriptional differences islets from male and female mice (n=9, 8) were
198 snap frozen and stored at -80°C until RNA extraction. To assess Tg-induced transcriptional
199 changes islets from each mouse were treated with DMSO or Tg for 6- or 12-hours in culture
200 media (11.1 mM D-glucose RPMI, 1% vol/vol P/S) (8 groups, n=3-4 per group, each n
201 represents pooled islet RNA from two mice). Islets were frozen at -80°C in 100 µL of RLT
202 buffer (Qiagen) with beta mercaptoethanol (1%). RNA was isolated using RNeasy Mini Kit
203 (Qiagen #74106) according to manufacturer's instructions. RNA sequencing was performed at
204 the UBC Biomedical Research Centre Sequencing Core. Sample quality control was
205 performed using the Agilent 2100 Bioanalyzer System (RNA Pico LabChip Kit). Qualifying
206 samples were prepped following the standard protocol for the NEBNext Ultra II Stranded
207 mRNA (New England Biolabs). Sequencing was performed on the Illumina NextSeq 500 with
208 Paired End 42bp × 42bp reads. Demultiplexed read sequences were then aligned to the
209 reference sequence (UCSC mm10) using STAR aligner (v 2.5.0b) (52). Gene differential
210 expression was analyzed using DESeq2 R package (53). Pathway enrichment analysis were
211 performed using Reactome (54). Over-representation analysis was performed using
212 NetworkAnalyst3.0 (www.networkanalyst.ca) (55).
213
214 **2.9. Proteomics**
215 Islets were treated with DMSO or Tg for 6 hours in islet culture media (11.1 mM D-glucose
216 RPMI, 1% vol/vol P/S) (4 groups, n=5-7 per group, each n represents pooled islets from two
217 mice). Islet pellets were frozen at -80°C in 100 µL of SDS lysis buffer (4% SDS, 100 mM Tris,
218 pH 8) and the proteins in each sample were precipitated using acetone. University of Victoria
219 proteomics service performed non-targeted quantitative proteomic analysis using data-
220 independent acquisition (DIA) with LC-MS/MS on an Orbitrap mass spectrometer. A mouse
221 FASTA database was downloaded from Uniprot (http://uniprot.org). This file was used with
222 the 6 gas phase fraction files from the analysis of the chromatogram library sample to create
223 a mouse islet specific chromatogram library using the EncyclopeDIA (v 1.2.2) software
224 package (Searle et al, 2018). This chromatogram library file was then used to perform
225 identification and quantitation of the proteins in the samples again using EncyclopeDIA with
226 Overlapping DIA as the acquisition type, trypsin used as the enzyme, CID/HCD as the
227 fragmentation, 10 ppm mass tolerances for the precursor, fragment, and library mass
228 tolerances. The Percolator version used was 3.10. The precursor FDR rate was set to 1%.
229 Protein abundances were log2 transformed, imputation was performed for missing values,

230 then proteins were normalized to median sample intensities. Gene differential expression was
231 analyzed using limma in Perseus (56).
232
233 ***2.10. Data from HPAP***
234 To compare sex differences in dynamic insulin secretion, data acquired was from the Human
235 Pancreas Analysis Program (HPAP-RRID:SCR_016202) Database
236 (https://hpap.pmacs.upenn.edu), a Human Islet Research Network (RRID:SCR_014393)
237 consortium (UC4-DK-112217, U01-DK-123594, UC4-DK-112232, and U01-DK-123716).
238
239 ***2.11. Statistical Analysis***
240 Statistical analyses and data presentation were carried out using GraphPad Prism 9
241 (GraphPad Software, San Diego, CA, USA) or R (v 4.1.1). Student's *t*-tests or two-way
242 ANOVAs were used for parametric data. A Mann-Whitney test was used for non-parametric
243 data. Statistical tests are indicated in the figure legends. For all statistical analyses,
244 differences were considered significant if the p-value was less than 0.05. *: $p<0.05$; ** $p<0.01$;
245 *** $p<0.001$. Data were presented as means ± SEM with individual data points from biological
246 replicates.
247
248
249 **3. Results**
250 ***3.1. Sex differences in β cell transcriptional and functional responses in ND and T2D***
251 ***human islets***
252 To define β cell-specific gene expression changes in T2D in each sex, we used a recently
253 compiled meta-analysis of publicly available scRNAseq datasets from male and female
254 human islets (57). In line with prior reports (12), non-diabetic (ND) and T2D β cells showed
255 significant transcriptional differences. In β cells isolated from female T2D donors, mRNA
256 levels of 127 genes were significantly different from ND female donors (77 downregulated, 50
257 upregulated in T2D) (Figure 1A-C). In β cells isolated from male T2D donors, 462 genes were
258 differentially expressed compared with male ND donors (138 downregulated, 324 upregulated
259 in T2D) (Figure 1A-C). Of the 660 genes that were differentially regulated in T2D, 71 were
260 differentially regulated in both males and females (15 downregulated, 56 upregulated in T2D)
261 (Figure 1A-C); however, the fold change for these 71 shared genes was different between
262 males and females (Figure S1A; Supplementary file 1). This suggests that for shared genes,

263 the magnitude of gene expression changes in T2D was not the same between the sexes.
264 Beyond shared genes, we observed that the majority of differentially expressed genes in T2D
265 (589/660) were unique to either males or females (Figure S1B, C; Supplementary file 1).
266 Given that the most prominent gene expression changes in T2D were found in genes that
267 were unique to one sex (Figure S2A, B; Supplementary file 1), these data suggest there are
268 important sex differences in the β cell gene expression response to T2D.
269 To determine which biological pathways were altered in β cells of T2D donors in each sex,
270 we performed pathway enrichment analysis. Genes that were upregulated in β cells isolated
271 from T2D donors included genes involved in Golgi-ER transport and the unfolded protein
272 response (UPR) pathways (Figure 1D-F; Supplementary file 1). While these biological
273 pathways were significantly upregulated in T2D in both males and females, ~75% of the
274 differentially regulated genes in these categories were unique to each sex (Table 1). Genes
275 that were downregulated in β cells from T2D donors revealed further differences between the
276 sexes: biological pathways downregulated in β cells from female T2D donors included cellular
277 responses to stress and to stimuli (Figure 1E; Supplementary file 1), whereas β cells from
278 male T2D donors showed downregulation of pathways associated with respiratory electron
279 transport and translation initiation (Figure 1F; Supplementary file 1). Thus, our analysis
280 suggests that sex-biased β cell gene expression responses to T2D may influence different
281 cellular processes in males and females.
282 The sex-biased β cell transcriptional response in T2D prompted us to compare glucose-
283 stimulated insulin secretion in each sex from ND and T2D human islets using data from the
284 Human Pancreas Analysis Program database (58). In ND donors, islets from males and
285 females showed similar patterns of insulin secretion in response to various stimulatory media
286 (Figure 1G, H). In donors living with T2D, we found that insulin secretion was impaired to a
287 greater degree in islets from males than in females (Figure 1G-K). Indeed, in male but not
288 female islets, insulin secretion was significantly lower in donors with T2D following stimulation
289 with both high glucose and IBMX (Figure 1I, J), which potentiates insulin secretion by
290 increasing cAMP levels to a similar degree as the incretins (59). Human islets from female
291 donors living with T2D therefore show better β insulin release than islets from males living
292 with T2D (Figure 1K). Indeed, while diabetes status was the main donor characteristic that
293 correlated with changes in insulin secretion (Figure S3A), we noted that in T2D sex and age
294 were two donor characteristics showing trends toward an effect on insulin secretion (Figure

295 S3B). Combined with our β cell gene expression data, these findings suggest that β cell
296 transcriptional and functional responses in T2D are not shared between the sexes.
297
298 ***3.2. Sex differences in UPR-associated gene expression in mouse islets***
299 Our unbiased analysis of human β cell gene expression and function in T2D revealed
300 differences between male and female donors living with T2D. Because human β cell gene
301 expression and function can be affected by factors such as peripheral insulin sensitivity,
302 disease processes, and medication (31,33), we investigated sex differences in β cell gene
303 expression and function in another context. We generated a well-powered islet RNAseq
304 dataset from 20-week-old male and female C57BL/6J mice, an age where we show insulin
305 sensitivity is equivalent between the sexes (Figure S4A). Principal component analysis and
306 unsupervised clustering clearly separated male and female islets on the basis of gene
307 expression (Figure 2A; Figure S5A). We found that 17.7% (3268/18938) of genes were
308 differentially expressed between the sexes (1648 upregulated in females, 1620 upregulated in
309 males), in line with estimates of sex-biased gene expression in other tissues (60,61).
310 Overrepresentation and pathway enrichment analysis both identified UPR-associated
311 pathways as a biological process that differed significantly between the sexes, where the
312 majority of genes in this category were enriched in female islets (Figure 2B, C;
313 Supplementary file 2). Additional genes that were enriched in female islets were those
314 associated with the gene ontology term “Cellular response to ER stress” (GO:0034976),
315 which included many genes involved in regulating protein synthesis (Figure 2D). For example,
316 females showed significantly higher levels of most ribosomal protein genes (Figure 2E).
317 Further genes enriched in females included those associated with protein folding, protein
318 processing, and quality control (Figure 2D). Given that protein synthesis, processing, and
319 folding capacity are intrinsically important for multiple islet cell types (62–65), including β cells
320 (66,67), this suggests female islets may have a larger protein production and folding capacity
321 than male islets.
322
323 ***3.3. Female islets are more resilient to endoplasmic reticulum stress in mice***
324 The burden of insulin production causes endoplasmic reticulum (ER) stress in β cells (68–70).
325 ER stress is associated with an attenuation of mRNA translation (71), and, if ER stress is
326 prolonged, can lead to cell death (72–74). Given that female islets exhibited higher
327 expression of genes associated with protein synthesis, processing, and folding than males,

328 and higher expression of genes associated with the UPR, which is activated in response to
329 ER stress (75), we examined global protein synthesis rates in male and female islets under
330 basal conditions and under ER stress. We incubated islets with O-propargyl-puromycin
331 (OPP), which is incorporated into newly-translated proteins and can be ligated to a
332 fluorophore. Using this technique, we monitored the accumulation of newly-synthesized islet
333 proteins with single-cell resolution (Figure S6A). In basal culture conditions, male islet cells
334 had significantly greater protein synthesis rates compared with female islet cells (Figure S6B).
335 To investigate islet protein synthesis under ER stress in each sex, we treated islets with
336 thapsigargin (Tg), a specific inhibitor of the sarcoplasmic/endoplasmic reticulum Ca^{2+}-ATPase
337 (SERCA) that induces ER stress and the UPR by lowering ER calcium levels (72,76). At 2
338 hours post-Tg treatment, protein synthesis was repressed in both male and female islet cells
339 (Figure 3A, B; Figure S6C). At 24 hours post-Tg treatment, we found that protein synthesis
340 was restored to basal levels in female islet cells, but not in male islet cells (Figure 3A, B;
341 Figure S6C). Importantly, recovery from protein synthesis repression was significantly
342 different in males and females (sex:treatment interaction p=0.0115). This suggests that while
343 protein synthesis repression associated with ER stress was transient in female islets, this
344 phenotype persisted for longer in male islets. Because insulin biosynthesis accounts for
345 approximately half the total protein production in β cells (77), one potential explanation for the
346 sex-specific recovery from protein synthesis repression is a sex difference in transcriptional
347 changes to insulin. To test this, we quantified GFP levels in β cells isolated from male and
348 female mice with GFP knocked into the endogenous mouse *Ins2* locus (*Ins2*$^{GFP/WT}$)(51,78).
349 While ER stress induced a significant reduction in *Ins2* gene activity, this response was
350 equivalent between the sexes. This suggests *Ins2* transcriptional changes cannot fully explain
351 the sex difference in recovery from protein synthesis repression during ER stress (Figure S7).
352 Given the prolonged protein synthesis repression in males following ER stress, we next
353 quantified cell death, another ER stress-associated phenotype (75), in male and female islets.
354 Using a kinetic cell death analysis, we observed clear sex differences in Tg-induced cell death
355 at 0.1 μM and 1.0 μM Tg doses throughout the time course of the experiment (Figure 3C, D).
356 After 84 hours of Tg treatment, no significant increase in female islet cell apoptosis was
357 observed with either 0.1 μM or 1.0 μM Tg treatment compared with controls (Figure 3E). In
358 contrast, cell death was significantly increased at both the 0.1 μM and the 1.0 μM doses of Tg
359 in male islet cells compared with vehicle-only controls (Figure 3F). Importantly, our analysis
360 shows the magnitude of Tg-induced cell death was larger in male islet cells compared with

361 female islet cells (sex:treatment interaction p=0.0399 [0.1 μM], p=0.0007 [1.0 μM]). While one
362 possible explanation for these data is that female islets are resistant to Tg-induced cell death,
363 we found a significant increase in apoptosis in both female and male islet cells treated with 10
364 μM Tg (Figure 3G, H, sex:treatment interaction p=0.0996 [0.1 μM]). This suggests female
365 islets were more resilient to mild ER stress caused by low-dose Tg than male islets.
366 To determine whether this increased ER stress resilience was caused by differential UPR
367 signaling, we monitored levels of several protein markers of UPR activation including binding
368 immunoglobulin protein (BiP), phosphorylated inositol-requiring enzyme 1 (pIRE1),
369 phosphorylated eukaryotic initiation factor alpha (peIF2α), and C/EBP homologous protein
370 (CHOP) (79,80) after treating male and female islets with 1 μM Tg for 24 hours. We found no
371 sex difference in UPR protein markers between male and female islets without Tg treatment
372 (Figure S8A-D) and observed a significant increase in levels of pIRE1α and CHOP in islets
373 from both sexes and BiP in female islets after a 24-hour Tg treatment (Figure S8A-D). Lack of
374 a sex difference in protein markers suggests UPR activation by Tg treatment was similar
375 between male and female islets at 20 weeks of age. While this finding differs from other
376 studies showing male-biased UPR activation (37), we reproduced the male-biased induction
377 of BiP in islets isolated from 60-week-old male and female mice (Figure S8E-G), suggesting
378 that age plays a role in the sex difference in UPR activation. Together, our data indicate that
379 despite equivalent UPR activation in male and female islets treated with Tg, significant sex
380 differences exist in ER stress-associated protein synthesis repression and cell death.
381
382 ***3.4. Female islets retain greater β cell function during ER stress in mice***
383 We next examined glucose-stimulated insulin secretion in islets cultured under basal
384 conditions and after Tg treatment (Figure 4A). In all conditions tested, high glucose
385 significantly stimulated insulin secretion in both sexes (Figure S9A); however, we identified
386 sex differences in how well islets sustained glucose-stimulated insulin secretion during longer
387 Tg treatments (Figure 4B, C, Figure S9A). Female islets, in both low and high glucose,
388 maintained robust insulin secretion during Tg treatment (Figure 4B). Specifically, we observed
389 a significant increase in insulin secretion after short Tg treatment (0 and 2 hours post-Tg),
390 with a return to basal secretion levels 4 hours post-Tg (Figure 4B). In contrast, male islets
391 showed no significant increase in insulin secretion after short Tg treatment, and there was a
392 significant drop in insulin secretion at 4 hours post-Tg treatment (Figure 4C). This suggests
393 female islets sustained insulin secretion for a longer period than male islets during ER stress.

394 Given that insulin content measurements showed insulin content significantly increased
395 during the 4-hour Tg treatment in female islets, but not male islets (Figure 4D), our data
396 suggest one reason female islets maintain insulin secretion during ER stress is by
397 augmenting islet insulin content. Proinsulin secretion followed similar trends to what we
398 observed with insulin secretion (Figure S9B), but Tg treatment reduced proinsulin content to a
399 greater degree in male islets (Figure 4E). This suggests that in addition to females
400 maintaining better insulin secretion during ER stress, they also show a larger increase in
401 insulin content and a smaller decrease in proinsulin content.
402 To determine whether female islets show improved β cell function under ER stress in other
403 contexts, we next monitored glucose-stimulated insulin secretion and glucose tolerance in
404 mice at 20 weeks, an age where we show insulin sensitivity was equivalent between the
405 sexes (Figure 4F-H; Figure S4). Despite higher fasting plasma insulin levels in males (Figure
406 4F), and similar glucose tolerance (Figure 4H), we found that the magnitude of glucose-
407 stimulated insulin secretion was greater in females (Figure 4G). Given that ER stress exists
408 even in normal physiological conditions due to the burden of insulin production (81), this adds
409 further support to a model in which female β cells maintain better insulin production than male
410 β cells under ER stress.
411
412 ***3.5. Sex differences in islet transcriptional and proteomic responses to ER stress in***
413 ***mice***
414 To gain insight into the differential ER stress-associated phenotypes in male and female
415 islets, we investigated global transcriptional changes after either a 6- or 12-hour Tg treatment
416 in each sex. Principal component analysis and unsupervised clustering shows that islets
417 clustered by sex, treatment, and treatment time (Figure 5A; Figure S10A). The majority of the
418 variance was explained by treatment (Figure 5B), and pathway enrichment analysis confirms
419 the UPR as the top upregulated pathway in Tg-treated male and female islets at both 6- and
420 12-hours after treatment (Figure S11A, B; Supplementary file 3). While some UPR-associated
421 genes differentially regulated by Tg treatment were shared between the sexes (6-hour: 29/36,
422 12-hour: 25/31), biological sex explained a large proportion of variance in the gene
423 expression response to ER stress. This suggests the transcriptional response to ER stress
424 was not fully shared between the sexes. Indeed, after a 6-hour Tg treatment, 32.6%
425 (2247/4655) of genes that were differentially expressed between DMSO and Tg were unique

426 to one sex (881 to females, 1376 to males). After a 12-hour Tg treatment, 29% (2259/7785)
427 were unique to one sex (1017 to males, 1242 to females).
428 To describe the transcriptional response of each sex to Tg treatment in more detail, we
429 used a two-way ANOVA to identify genes that were upregulated, downregulated, or
430 unchanged in male and female islets between 6- and 12-hours post-Tg (Supplementary file
431 4). By performing pathway enrichment analysis, we were able to determine which processes
432 were shared, and which processes differed, between the sexes during Tg treatment. For
433 example, we observed a significant increase in mRNA levels of genes corresponding to
434 pathways such as cellular responses to stimuli, stress, and starvation in both male and female
435 islets between 6- and 12-hour Tg treatments (Figure 5C; Supplementary file 4), suggesting Tg
436 has similar effects on genes related to these pathways in both sexes. In contrast, there was a
437 male-specific increase in mRNA levels of genes associated with translation during Tg
438 treatment (Figure 5C; Supplementary file 4). In females, there was a decrease in mRNA
439 levels of genes associated with β cell identity, such as *Pklr*, *Rfx6*, *Hnf4a*, *Slc2a2*, *Pdx1*, and
440 *MafA* (Figure S12A), and in genes linked with regulation of gene expression in β cells (Figure
441 5C). Neither of these categories were altered between 6- and 12-hour Tg treatments in males
442 (Figure 5C; Figure S12B). While this data suggests some aspects of the gene expression
443 response to ER stress were shared between the sexes, we found that many genes
444 corresponding to important cellular processes were differentially regulated during Tg
445 treatment in only one sex.
446 Beyond sex-specific transcriptional changes following Tg treatment, ER stress also had a
447 sex-specific effect on the islet proteome. Although the majority of proteins were
448 downregulated by Tg treatment due to the generalized repression of protein synthesis under
449 ER stress (Figure 5D), we identified 47 proteins (35 downregulated, 12 upregulated in Tg)
450 that were differentially expressed in female islets and 82 proteins (72 downregulated, 10
451 upregulated in Tg) that were differentially expressed after Tg treatment in male islets
452 (Supplementary table 1). Proteins downregulated only in females include proteins associated
453 with GO term 'endoplasmic reticulum to Golgi vesicle-mediated transport' (GO:0006888)
454 (BCAP31, COG5, COG3, GOSR1), whereas proteins downregulated only in males include
455 proteins associated with GO terms 'insulin secretion' (GO:0030073) (PTPRN2, CLTRN,
456 PTPRN) and 'lysosome pathway' (KEGG) (NPC2, CTSZ, LAMP2, PSAP, CLTA). Importantly,
457 only seven differentially expressed proteins were in common between the sexes (Figure 5D).

458 This suggests that as with our phenotypic and transcriptomic data, the proteomic response to
459 Tg treatment was largely not shared between the sexes.
460
461
462 **4. Discussion**
463 Emerging evidence shows biological sex affects many aspects of β cell gene expression and
464 function. Yet, many studies on β cells do not include both sexes, or fail to analyze male and
465 female data separately. To address this gap in knowledge, the goal of our study was to
466 provide detailed information on sex differences in islet and β cell gene expression and
467 function in multiple contexts. In humans, we used a large scRNAseq dataset from ND and
468 T2D donors to reveal significant male-female differences in the magnitude of gene expression
469 changes, and in the identity of genes that were differentially regulated, between ND and T2D
470 donors. This suggests β cell gene expression changes in T2D are not fully shared between
471 the sexes. Given that our analysis shows β cells from female donors living with T2D maintain
472 better insulin production than β cells from male donors living with T2D, our findings suggest
473 female β cells are more resilient than male β cells in the context of T2D. In mice, our
474 unbiased analysis of gene expression in islets from males and females with equivalent insulin
475 sensitivity revealed sex differences in genes associated with the UPR under normal
476 physiological conditions. This differential gene expression was significant, as female islets
477 were more resilient to phenotypes caused by ER stress and UPR activation than male islets,
478 showed sex-specific transcriptional and proteomic changes in this context, and maintained
479 better insulin secretion. Collectively, these data suggest that in rodents, β cells from females
480 are more resilient to ER stress. Considering the well-established links between ER stress and
481 T2D (79,82–84), our data suggests a model in which female β cells maintain better function in
482 T2D because they are more resilient to ER stress and UPR activation. While future studies
483 are needed to test this model, and to assess the relative contribution of sex differences in β
484 cells to the sex-biased risk of T2D, our findings highlight the importance of including both
485 sexes in islet and β cell studies.
486 With respect to gene expression, including both sexes in our analysis of β cell gene
487 expression in human ND and T2D allowed us to uncover genes that were differentially
488 regulated in T2D in each sex. Because many of these genes may have been missed if the
489 scRNAseq data was not analyzed by sex, our findings advance knowledge of β cell changes
490 in T2D by identifying additional genes that are differentially regulated in this context. This

491 knowledge adds to a growing number of studies that identify sex differences in β cell gene
492 expression during aging in humans (12), and in mice fed either a normal (4,11) or a high fat
493 diet (11). Further, given that our RNAseq on islets from male and female mice with equivalent
494 insulin sensitivity identifies genes and biological pathways that align with previous studies on
495 sex differences in murine β cell gene expression (4,11), our data suggests that sex
496 differences in islet and β cell gene expression cannot be explained solely by a male-female
497 difference in peripheral insulin resistance. Instead, there is likely a basal sex difference in β
498 cell gene expression that forms the foundation for sex-specific transcriptional responses to
499 perturbations such as ER stress and T2D. By generating large gene expression datasets from
500 islet from male and female mice with equivalent peripheral insulin sensitivity and from islets
501 subjected to pharmacological induction of ER stress, our studies provide a foundation of
502 knowledge for future studies aimed at studying the causes and consequences of sex
503 differences in islet ER stress responses and β cell function following UPR activation. This will
504 provide deeper mechanistic insight into the sex-specific phenotypic effects reported in animal
505 models of β cell dysfunction (35–39,85–88) and the sex-biased risk of diseases such as T2D
506 that are associated with β cell dysfunction (12,22,89,90).
507 Beyond gene expression, our sex-based analysis of mouse islets allowed us to uncover
508 male-female differences in ER stress-associated phenotypes (*e.g*. protein synthesis
509 repression, cell death). While previous studies identify a sex difference in β cell loss in
510 diabetic mouse models (37,39,91), and show that estrogen plays a protective role via
511 estrogen receptor α (ERα) against ER stress to preserve β cell mass and prevent apoptosis in
512 cell lines, mouse models, and human islets (39,91,92), we extend prior findings by showing
513 that differences in ER stress-induced cell death were present in the context of equivalent
514 insulin sensitivity between the sexes. This suggests sex differences in ER stress-associated
515 phenotypes occur prior to male-female differences in peripheral insulin sensitivity. Indeed,
516 islets isolated from males and females with equivalent sensitivity also show a sex difference
517 in protein synthesis repression, a classical ER stress-associated phenotype (75). While
518 estrogen affects insulin biosynthesis via ERα (93), future studies will need to determine
519 whether estrogen also allows female islets to restore protein synthesis to basal levels faster
520 than male islets following ER stress. We currently lack this knowledge, as most studies on
521 UPR-mediated recovery from protein translation repression use single- and mixed-sex animal
522 groups, or cultured cells (94–99).

523 Assessing whether the recovery of protein synthesis contributes to reduced cell death in
524 female islets following ER stress will also be an important task for future studies, as prior
525 studies suggest the inability to recover from protein synthesis repression increases ER-stress
526 induced apoptosis (94). Ideally, this type of study would also monitor the activity of pathways
527 known to regulate protein synthesis repression during ER stress. For example, while we did
528 not detect any changes in levels of phosphorylated eIF2α (also known as Eif2s1), which is
529 known to mediate UPR-induced protein synthesis repression (75), our chosen timepoints did
530 not overlap with the rapid changes in phospho-eIF2α following ER stress published in other
531 studies (100,101). A more detailed time course will therefore be necessary to assess p-eIF2α
532 levels during ER stress in both sexes, and to test a role for phospho-eIF2α in mediating
533 differences in protein synthesis repression. Ultimately, a better understanding of sex
534 differences in ER stress-associated phenotypes in β cells will provide a mechanistic
535 explanation for the strongly male-biased onset of diabetes-like phenotypes in mouse models
536 of β cell ER stress (*e.g.* Akita, KINGS, Munich mice) (37,38,85). Given the known relationship
537 between ER stress, β cell death, and T2D, studies on the male-female difference in β cell ER
538 stress-associated phenotypes may also advance our understanding of the male-biased risk of
539 developing T2D in some population groups.
540 A further benefit of additional studies on the sex difference in β cell ER stress responses
541 will be to identify mechanisms that support β cell insulin production. In rodents, we found that
542 female islets maintained high glucose-stimulated insulin secretion and increased insulin
543 content following ER stress, whereas male islets showed significant repression of high
544 glucose-stimulated insulin secretion under the same conditions. In humans, while a study
545 using a mixed-sex group of T2D donors shows β cells experience ER stress associated with β
546 cell dysfunction (102), we found that changes to β cell insulin secretion in T2D were not the
547 same between the sexes. Specifically, the magnitude of the reduction in insulin release by β
548 cells from female donors living with T2D was smaller than in β cells from male donors living
549 with T2D. Together with our data from rodents, this suggests female β cells maintain
550 enhanced insulin production and/or secretion in multiple contexts, and the increased β cell
551 function cannot be solely attributed to a sex difference in peripheral insulin sensitivity.
552 Clues into potential ways that female β cells maintain improved insulin production and
553 secretion emerge from our examination of the transcriptional response to ER stress in each
554 sex. Our data shows that Tg treatment induces gene expression changes characteristic of ER
555 stress (103), and revealed similar biological pathways that were upregulated in T2D donors.

556 Furthermore, we identified significant differences between male and female islets in the
557 transcriptional response to ER stress over time. One notable finding was that a greater
558 number of β cell identity genes were downregulated between 6- and 12-hour Tg treatments in
559 females, but not in males. Because most studies on the relationship between β cell identity
560 and function used a mixed-sex pool of islets and β cells (68,104,105), more studies will be
561 needed to test whether there are sex-specific changes to β cell identity during ER stress, and
562 to determine the functional consequences of this sex-specific effect. Ultimately, a better
563 understanding of changes to β cell gene expression and function in males and females will
564 suggest effective ways to reverse disease-associated changes to this important cell type in
565 each sex, improving equity in health outcomes (106).
566

567 **4.1. Conclusions**

568 Our study reports significant sex differences in islet and β cell gene expression and stress
569 responses in both humans and mice. These differences likely contribute to sex differences in
570 β cell resilience, allowing female β cells to maintain better insulin production across multiple
571 contexts. This knowledge forms a foundation for future studies aimed at understanding how
572 sex differences β cell function affect physiology and the pathophysiology of diseases such as
573 T2D.
574

575 **Funding**

576 This study was supported by operating grants to E.J.R. from the Michael Smith Foundation for
577 Health Research (16876), Canadian Institutes of Health Research (GS4-171365), the
578 Canadian Foundation for Innovation (JELF-34879), and to J.D.J. (PJT-152999) from the
579 Canadian Institutes of Health Research, and core support from the JDRF Centre of
580 Excellence at UBC (3-COE-2022-1103-M-B). J.D.J. was funded by a Diabetes Investigator
581 Award from Diabetes Canada.
582
583

584 **Acknowledgements**

585 We thank members of the Rideout and Johnson lab for valuable feedback. We thank our
586 animal care staff for supporting our animal husbandry, UBC Biomedical Research Center for
587 performing RNA sequencing, and UVic Genome BC Proteomics Center for performing

proteomics. We acknowledge that our research takes place on the traditional, ancestral, and unceded territory of the Musqueam people; a privilege for which we are grateful.

Conflict of interest

The authors declare no competing interest.

Data Availability

Details of all statistical tests and *p*-values are provided in Supplementary file 5. All raw data generated in this study are available in Supplementary file 6. RNAseq data is available in Supplementary file 7 and Supplementary file 8.

REFERENCES

1. Parchami A, Kusha S. Effect of sex on histomorphometric properties of Langerhans islets in native chickens. Vet Res Forum. 2015;6(4):327–30.

2. Rideout EJ, Narsaiya MS, Grewal SS. The Sex Determination Gene transformer Regulates Male-Female Differences in Drosophila Body Size. PLOS Genet. 2015 Dec 28;11(12):e1005683.

3. Millington JW, Brownrigg GP, Chao C, Sun Z, Basner-Collins PJ, Wat LW, et al. Female-biased upregulation of insulin pathway activity mediates the sex difference in Drosophila body size plasticity. eLife. 2021 Jan 15;10:e58341.

4. Stancill JS, Osipovich AB, Cartailler JP, Magnuson MA. Transgene-associated human growth hormone expression in pancreatic β-cells impairs identification of sex-based gene expression differences. Am J Physiol Endocrinol Metab. 2019 Feb 1;316(2):E196–209.

5. Horie I, Abiru N, Eto M, Sako A, Akeshima J, Nakao T, et al. Sex differences in insulin and glucagon responses for glucose homeostasis in young healthy Japanese adults. J Diabetes Investig. 2018 Nov;9(6):1283–7.

6. Marchese E, Rodeghier C, Monson RS, McCracken B, Shi T, Schrock W, et al. Enumerating β-Cells in Whole Human Islets: Sex Differences and Associations With Clinical Outcomes After Islet Transplantation. Diabetes Care. 2015 Nov 1;38(11):e176–7.

7. Oliva M, Muñoz-Aguirre M, Kim-Hellmuth S, Wucher V, Gewirtz ADH, Cotter DJ, et al. The impact of sex on gene expression across human tissues. Science [Internet]. 2020 Sep 11 [cited 2022 Feb 3]; Available from: https://www.science.org/doi/abs/10.1126/science.aba3066

8. Enge M, Arda HE, Mignardi M, Beausang J, Bottino R, Kim SK, et al. Single-Cell Analysis of Human Pancreas Reveals Transcriptional Signatures of Aging and Somatic Mutation Patterns. Cell. 2017 Oct 5;171(2):321-330.e14.

625 9. Schaum N, Lehallier B, Hahn O, Pálovics R, Hosseinzadeh S, Lee SE, et al. Aging hallmarks
626 exhibit organ-specific temporal signatures. Nature. 2020 Jul;583(7817):596–602.

627 10. Hall E, Volkov P, Dayeh T, Esguerra JLS, Salö S, Eliasson L, et al. Sex differences in the
628 genome-wide DNA methylation pattern and impact on gene expression, microRNA levels and
629 insulin secretion in human pancreatic islets. Genome Biol. 2014 Dec 3;15(12):522.

630 11. Liu G, Li Y, Zhang T, Li M, Li S, He Q, et al. Single-cell RNA Sequencing Reveals Sexually
631 Dimorphic Transcriptome and Type 2 Diabetes Genes in Mouse Islet β Cells. Genomics
632 Proteomics Bioinformatics. 2021 Jun 1;19(3):408–22.

633 12. Arrojo e Drigo R, Erikson G, Tyagi S, Capitanio J, Lyon J, Spigelman AF, et al. Aging of human
634 endocrine pancreatic cell types is heterogeneous and sex-specific [Internet]. Physiology; 2019
635 Aug [cited 2021 Jun 20]. Available from: http://biorxiv.org/lookup/doi/10.1101/729541

636 13. Li T, Jiao W, Li W, Li H. Sex effect on insulin secretion and mitochondrial function in pancreatic
637 beta cells of elderly Wistar rats. Endocr Res. 2016 Jul 2;41(3):167–79.

638 14. Tura A, Pacini G, Moro E, Vrbíková J, Bendlová B, Kautzky-Willer A. Sex- and age-related
639 differences of metabolic parameters in impaired glucose metabolism and type 2 diabetes
640 compared to normal glucose tolerance. Diabetes Res Clin Pract. 2018 Dec 1;146:67–75.

641 15. Kautzky-Willer A, Brazzale AR, Moro E, Vrbíková J, Bendlova B, Sbrignadello S, et al. Influence
642 of Increasing BMI on Insulin Sensitivity and Secretion in Normotolerant Men and Women of a
643 Wide Age Span. Obesity. 2012;20(10):1966–73.

644 16. Basu R, Man CD, Campioni M, Basu A, Klee G, Toffolo G, et al. Effects of Age and Sex on
645 Postprandial Glucose Metabolism: Differences in Glucose Turnover, Insulin Secretion, Insulin
646 Action, and Hepatic Insulin Extraction. Diabetes. 2006 Jul 1;55(7):2001–14.

647 17. Nuutila P, Knuuti MJ, Mäki M, Laine H, Ruotsalainen U, Teräs M, et al. Gender and Insulin
648 Sensitivity in the Heart and in Skeletal Muscles: Studies Using Positron Emission Tomography.
649 Diabetes. 1995 Jan 1;44(1):31–6.

650 18. Lundsgaard AM, Kiens B. Gender Differences in Skeletal Muscle Substrate Metabolism –
651 Molecular Mechanisms and Insulin Sensitivity. Front Endocrinol [Internet]. 2014 [cited 2022 Apr
652 27];5. Available from: https://www.frontiersin.org/article/10.3389/fendo.2014.00195

653 19. Borissova AM, Tankova T, Kirilov G, Koev D. Gender-dependent effect of ageing on peripheral
654 insulin action. Int J Clin Pract. 2005;59(4):422–6.

655 20. Geer EB, Shen W. Gender differences in insulin resistance, body composition, and energy
656 balance. Gend Med. 2009 Jan 1;6:60–75.

657 21. Færch K, Borch-Johnsen K, Vaag A, Jørgensen T, Witte DR. Sex differences in glucose levels: a
658 consequence of physiology or methodological convenience? The Inter99 study. Diabetologia.
659 2010 May 1;53(5):858–65.

660 22. Gannon M, Kulkarni RN, Tse HM, Mauvais-Jarvis F. Sex differences underlying pancreatic islet
661 biology and its dysfunction. Mol Metab. 2018 Sep;15:82–91.

662 23. Tramunt B, Smati S, Grandgeorge N, Lenfant F, Arnal JF, Montagner A, et al. Sex differences in
663 metabolic regulation and diabetes susceptibility. Diabetologia [Internet]. 2019 Nov 21 [cited 2019
664 Dec 4]; Available from: https://doi.org/10.1007/s00125-019-05040-3

665 24. Macotela Y, Boucher J, Tran TT, Kahn CR. Sex and Depot Differences in Adipocyte Insulin
666 Sensitivity and Glucose Metabolism. Diabetes. 2009 Apr;58(4):803–12.

667 25. Rudnicki M, Abdifarkosh G, Rezvan O, Nwadozi E, Roudier E, Haas TL. Female Mice Have
668 Higher Angiogenesis in Perigonadal Adipose Tissue Than Males in Response to High-Fat Diet.
669 Front Physiol [Internet]. 2018 [cited 2022 May 5];9. Available from:
670 https://www.frontiersin.org/article/10.3389/fphys.2018.01452

671 26. Millington JW, Biswas P, Chao C, Xia YH, Wat LW, Brownrigg GP, et al. A low sugar diet
672 enhances Drosophila body size in males and females via sex-specific mechanisms. Dev Camb
673 Engl. 2022 Feb 23;dev.200491.

674 27. Mank JE, Rideout EJ. Developmental mechanisms of sex differences: from cells to organisms.
675 Development. 2021 Oct 14;148(19):dev199750.

676 28. Oster RT, Johnson JA, Hemmelgarn BR, King M, Balko SU, Svenson LW, et al. Recent
677 epidemiologic trends of diabetes mellitus among status Aboriginal adults. CMAJ Can Med Assoc
678 J. 2011 Sep 6;183(12):E803–8.

679 29. Dyck R, Osgood N, Lin TH, Gao A, Stang MR. Epidemiology of diabetes mellitus among First
680 Nations and non-First Nations adults. CMAJ Can Med Assoc J. 2010 Feb 23;182(3):249–56.

681 30. Zhou B, Lu Y, Hajifathalian K, Bentham J, Cesare MD, Danaei G, et al. Worldwide trends in
682 diabetes since 1980: a pooled analysis of 751 population-based studies with 4·4 million
683 participants. The Lancet. 2016 Apr 9;387(10027):1513–30.

684 31. Kautzky-Willer A, Harreiter J, Pacini G. Sex and Gender Differences in Risk, Pathophysiology
685 and Complications of Type 2 Diabetes Mellitus. Endocr Rev. 2016 Jun;37(3):278–316.

686 32. Heise L, Greene ME, Opper N, Stavropoulou M, Harper C, Nascimento M, et al. Gender
687 inequality and restrictive gender norms: framing the challenges to health. Lancet Lond Engl. 2019
688 Jun 15;393(10189):2440–54.

689 33. Kautzky-Willer A, Harreiter J. Sex and gender differences in therapy of type 2 diabetes. Diabetes
690 Res Clin Pract. 2017 Sep;131:230–41.

691 34. Corsetti JP, Sparks JD, Peterson RG, Smith RL, Sparks CE. Effect of dietary fat on the
692 development of non-insulin dependent diabetes mellitus in obese Zucker diabetic fatty male and
693 female rats. Atherosclerosis. 2000 Feb;148(2):231–41.

694 35. Paik SG, Michelis MA, Kim YT, Shin S. Induction of insulin-dependent diabetes by streptozotocin.
695 Inhibition by estrogens and potentiation by androgens. Diabetes. 1982 Aug;31(8 Pt 1):724–9.

696 36. Verchere CB, D'Alessio DA, Palmiter RD, Weir GC, Bonner-Weir S, Baskin DG, et al. Islet
697 amyloid formation associated with hyperglycemia in transgenic mice with pancreatic beta cell
698 expression of human islet amyloid polypeptide. Proc Natl Acad Sci U S A. 1996 Apr
699 16;93(8):3492–6.

700 37. Austin ALF, Daniels Gatward LF, Cnop M, Santos G, Andersson D, Sharp S, et al. The KINGS
701 Ins2+/G32S Mouse: A Novel Model of β-Cell Endoplasmic Reticulum Stress and Human
702 Diabetes. Diabetes. 2020 Dec;69(12):2667–77.

703 38. Yoshioka M, Kayo T, Ikeda T, Koizuni A. A Novel Locus, Mody4, Distal to D7Mit189 on
704 Chromosome 7 Determines Early-Onset NIDDM in Nonobese C57BL/6 (Akita) Mutant Mice.
705 Diabetes. 1997 May 1;46(5):887–94.

706 39. May CL, Chu K, Hu M, Ortega CS, Simpson ER, Korach KS, et al. Estrogens protect pancreatic
707 β-cells from apoptosis and prevent insulin-deficient diabetes mellitus in mice. Proc Natl Acad Sci
708 U S A. 2006 Jun 13;103(24):9232.

709 40. Cohrs CM, Panzer JK, Drotar DM, Enos SJ, Kipke N, Chen C, et al. Dysfunction of Persisting β
710 Cells Is a Key Feature of Early Type 2 Diabetes Pathogenesis. Cell Rep. 2020 Apr
711 7;31(1):107469.

712 41. Saisho Y. β-cell dysfunction: Its critical role in prevention and management of type 2 diabetes.
713 World J Diabetes. 2015 Feb 15;6(1):109–24.

714 42. Segerstolpe Å, Palasantza A, Eliasson P, Andersson EM, Andréasson AC, Sun X, et al. Single-
715 Cell Transcriptome Profiling of Human Pancreatic Islets in Health and Type 2 Diabetes. Cell
716 Metab. 2016 Oct 11;24(4):593–607.

717 43. Xin Y, Kim J, Okamoto H, Ni M, Wei Y, Adler C, et al. RNA Sequencing of Single Human Islet
718 Cells Reveals Type 2 Diabetes Genes. Cell Metab. 2016 Oct 11;24(4):608–15.

719 44. Avrahami D, Wang YJ, Schug J, Feleke E, Gao L, Liu C, et al. Single-cell transcriptomics of
720 human islet ontogeny defines the molecular basis of β-cell dedifferentiation in T2D. Mol Metab.
721 2020 Jul 30;42:101057.

722 45. Lawlor N, George J, Bolisetty M, Kursawe R, Sun L, Sivakamasundari V, et al. Single-cell
723 transcriptomes identify human islet cell signatures and reveal cell-type–specific expression
724 changes in type 2 diabetes. Genome Res. 2017 Feb 1;27(2):208–22.

725 46. Baron M, Veres A, Wolock SL, Faust AL, Gaujoux R, Vetere A, et al. A Single-Cell
726 Transcriptomic Map of the Human and Mouse Pancreas Reveals Inter- and Intra-cell Population
727 Structure. Cell Syst. 2016 Oct 26;3(4):346-360.e4.

728 47. Muraro MJ, Dharmadhikari G, Grün D, Groen N, Dielen T, Jansen E, et al. A Single-Cell
729 Transcriptome Atlas of the Human Pancreas. Cell Syst. 2016 Oct 26;3(4):385-394.e3.

730 48. Deng S, Vatamaniuk M, Huang X, Doliba N, Lian MM, Frank A, et al. Structural and Functional
731 Abnormalities in the Islets Isolated From Type 2 Diabetic Subjects. Diabetes. 2004 Mar
732 1;53(3):624–32.

733 49. Wu M, Lee MYY, Bahl V, Traum D, Schug J, Kusmartseva I, et al. Single-cell analysis of the
734 human pancreas in type 2 diabetes using multi-spectral imaging mass cytometry. Cell Rep. 2021
735 Nov 2;37(5):109919.

736 50. Salvalaggio PRO, Deng S, Ariyan CE, Millet I, Zawalich WS, Basadonna GP, et al. Islet filtration:
737 a simple and rapid new purification procedure that avoids ficoll and improves islet mass and
738 function. Transplantation. 2002 Sep 27;74(6):877–9.

739 51. Chu CMJ, Modi H, Skovsø S, Ellis C, Krentz NAJ, Zhao YB, et al. Dynamic Ins2 gene activity
740 defines β-cell maturity states [Internet]. bioRxiv; 2022 [cited 2022 Oct 6]. p. 702589. Available
741 from: https://www.biorxiv.org/content/10.1101/702589v3

742 52. Dobin A, Davis CA, Schlesinger F, Drenkow J, Zaleski C, Jha S, et al. STAR: ultrafast universal
743 RNA-seq aligner. Bioinforma Oxf Engl. 2013 Jan 1;29(1):15–21.

744 53. Love MI, Huber W, Anders S. Moderated estimation of fold change and dispersion for RNA-seq
745 data with DESeq2. Genome Biol. 2014 Dec 5;15(12):550.

746 54. Gillespie M, Jassal B, Stephan R, Milacic M, Rothfels K, Senff-Ribeiro A, et al. The reactome
747 pathway knowledgebase 2022. Nucleic Acids Res. 2022 Jan 7;50(D1):D687–92.

748 55. Zhou G, Soufan O, Ewald J, Hancock REW, Basu N, Xia J. NetworkAnalyst 3.0: a visual
749 analytics platform for comprehensive gene expression profiling and meta-analysis. Nucleic Acids
750 Res. 2019 Jul 2;47(W1):W234–41.

751 56. Tyanova S, Temu T, Sinitcyn P, Carlson A, Hein MY, Geiger T, et al. The Perseus computational
752 platform for comprehensive analysis of (prote)omics data. Nat Methods. 2016 Sep;13(9):731–40.

753 57. Wang S, Flibotte S, Camunas-Soler J, MacDonald PE, Johnson JD. A New Hypothesis for Type
754 1 Diabetes Risk: The At-Risk Allele at rs3842753 Associates With Increased Beta-Cell INS
755 Messenger RNA in a Meta-Analysis of Single-Cell RNA-Sequencing Data. Can J Diabetes. 2021
756 Dec 1;45(8):775-784.e2.

757 58. Kaestner KH, Powers AC, Naji A, HPAP Consortium, Atkinson MA. NIH Initiative to Improve
758 Understanding of the Pancreas, Islet, and Autoimmunity in Type 1 Diabetes: The Human
759 Pancreas Analysis Program (HPAP). Diabetes. 2019 Jul;68(7):1394–402.

760 59. Hellman B, Idahl LÅ, Lernmark Å, Täljedal IB. The Pancreatic β-Cell Recognition of Insulin
761 Secretagogues: Does Cyclic AMP Mediate the Effect of Glucose? Proc Natl Acad Sci. 1974
762 Sep;71(9):3405–9.

763 60. Yang X, Schadt EE, Wang S, Wang H, Arnold AP, Ingram-Drake L, et al. Tissue-specific
764 expression and regulation of sexually dimorphic genes in mice. Genome Res. 2006 Aug
765 1;16(8):995–1004.

766 61. Lu T, Mar JC. Investigating transcriptome-wide sex dimorphism by multi-level analysis of single-
767 cell RNA sequencing data in ten mouse cell types. Biol Sex Differ. 2020 Nov 5;11(1):61.

768 62. Cottet-Dumoulin D, Lavallard V, Lebreton F, Wassmer CH, Bellofatto K, Parnaud G, et al.
769 Biosynthetic Activity Differs Between Islet Cell Types and in Beta Cells Is Modulated by Glucose
770 and Not by Secretion. Endocrinology. 2020 Dec 25;162(3):bqaa239.

771 63. Li N, Yang Z, Li Q, Yu Z, Chen X, Li JC, et al. Ablation of somatostatin cells leads to impaired
772 pancreatic islet function and neonatal death in rodents. Cell Death Dis. 2018 Jun 7;9(6):1–12.

773 64. Webb GC, Dey A, Wang J, Stein J, Milewski M, Steiner DF. Altered Proglucagon Processing in
774 an α-Cell Line Derived from Prohormone Convertase 2 Null Mouse Islets*. J Biol Chem. 2004 Jul
775 23;279(30):31068–75.

776 65. Garcia-Barrado MJ, Ravier MA, Rolland JF, Gilon P, Nenquin M, Henquin JC. Inhibition of
777 Protein Synthesis Sequentially Impairs Distinct Steps of Stimulus-secretion Coupling in
778 Pancreatic β Cells. Endocrinology. 2001 Jan 1;142(1):299–307.

779 66. Scheuner D, Mierde DV, Song B, Flamez D, Creemers JWM, Tsukamoto K, et al. Control of
780 mRNA translation preserves endoplasmic reticulum function in beta cells and maintains glucose
781 homeostasis. Nat Med. 2005 Jul;11(7):757–64.

782 67. Izumi T, Yokota-Hashimoto H, Zhao S, Wang J, Halban PA, Takeuchi T. Dominant negative
783 pathogenesis by mutant proinsulin in the Akita diabetic mouse. Diabetes. 2003 Feb;52(2):409–
784 16.

785 68. Xin Y, Dominguez Gutierrez G, Okamoto H, Kim J, Lee AH, Adler C, et al. Pseudotime Ordering
786 of Single Human β-Cells Reveals States of Insulin Production and Unfolded Protein Response.
787 Diabetes. 2018;67(9):1783–94.

788 69. Lipson KL, Fonseca SG, Ishigaki S, Nguyen LX, Foss E, Bortell R, et al. Regulation of insulin
789 biosynthesis in pancreatic beta cells by an endoplasmic reticulum-resident protein kinase IRE1.
790 Cell Metab. 2006 Sep;4(3):245–54.

791 70. Teodoro T, Odisho T, Sidorova E, Volchuk A. Pancreatic β-cells depend on basal expression of
792 active ATF6α-p50 for cell survival even under nonstress conditions. Am J Physiol-Cell Physiol.
793 2012 Apr;302(7):C992–1003.

794 71. Scheuner D, Song B, McEwen E, Liu C, Laybutt R, Gillespie P, et al. Translational control is
795 required for the unfolded protein response and in vivo glucose homeostasis. Mol Cell. 2001
796 Jun;7(6):1165–76.

797 72. Luciani DS, Gwiazda KS, Yang TLB, Kalynyak TB, Bychkivska Y, Frey MHZ, et al. Roles of IP3R
798 and RyR Ca2+ Channels in Endoplasmic Reticulum Stress and β-Cell Death. Diabetes. 2009
799 Feb 1;58(2):422–32.

800 73. Riggs AC, Bernal-Mizrachi E, Ohsugi M, Wasson J, Fatrai S, Welling C, et al. Mice conditionally
801 lacking the Wolfram gene in pancreatic islet beta cells exhibit diabetes as a result of enhanced
802 endoplasmic reticulum stress and apoptosis. Diabetologia. 2005 Nov 1;48(11):2313–21.

803 74. Li J, Lee B, Lee AS. Endoplasmic reticulum stress-induced apoptosis: multiple pathways and
804 activation of p53-up-regulated modulator of apoptosis (PUMA) and NOXA by p53. J Biol Chem.
805 2006 Mar 17;281(11):7260–70.

806 75. Sharma RB, Landa-Galván HV, Alonso LC. Living Dangerously: Protective and Harmful ER
807 Stress Responses in Pancreatic β-Cells. Diabetes. 2021 Nov;70(11):2431.

808 76. Gwiazda KS, Yang TLB, Lin Y, Johnson JD. Effects of palmitate on ER and cytosolic Ca2+
809 homeostasis in β-cells. Am J Physiol-Endocrinol Metab. 2009 Apr;296(4):E690–701.

810 77. Fonseca SG, Gromada J, Urano F. Endoplasmic reticulum stress and pancreatic beta cell death.
811 Trends Endocrinol Metab TEM. 2011 Jul;22(7):266–74.

812 78. Wakae-Takada N, Xuan S, Watanabe K, Meda P, Leibel RL. Molecular basis for the regulation of
813 islet beta cell mass in mice: the role of E-cadherin. Diabetologia. 2013 Apr;56(4):856–66.

814 79. Shrestha N, Franco ED, Arvan P, Cnop M. Pathological β-Cell Endoplasmic Reticulum Stress in
815 Type 2 Diabetes: Current Evidence. Front Endocrinol [Internet]. 2021 [cited 2022 Jan 26];12.
816 Available from: https://www.ncbi.nlm.nih.gov/labs/pmc/articles/PMC8101261/

817 80. Oyadomari S, Mori M. Roles of CHOP/GADD153 in endoplasmic reticulum stress. Cell Death
818 Differ. 2004 Apr;11(4):381–9.

819 81. Szabat M, Page MM, Panzhinskiy E, Skovsø S, Mojibian M, Fernandez-Tajes J, et al. Reduced
820 Insulin Production Relieves Endoplasmic Reticulum Stress and Induces β Cell Proliferation. Cell
821 Metab. 2016 Jan 12;23(1):179–93.

822 82. Laybutt DR, Preston AM, Åkerfeldt MC, Kench JG, Busch AK, Biankin AV, et al. Endoplasmic
823 reticulum stress contributes to beta cell apoptosis in type 2 diabetes. Diabetologia. 2007 Apr
824 1;50(4):752–63.

825 83. Engin F, Nguyen T, Yermalovich A, Hotamisligil GS. Aberrant islet unfolded protein response in
826 type 2 diabetes. Sci Rep. 2014 Feb 11;4(1):4054.

827 84. Huang C jiang, Lin C yu, Haataja L, Gurlo T, Butler AE, Rizza RA, et al. High expression rates of
828 human islet amyloid polypeptide induce endoplasmic reticulum stress mediated beta-cell
829 apoptosis, a characteristic of humans with type 2 but not type 1 diabetes. Diabetes. 2007
830 Aug;56(8):2016–27.

831 85. Herbach N, Rathkolb B, Kemter E, Pichl L, Klaften M, de Angelis MH, et al. Dominant-Negative
832 Effects of a Novel Mutated Ins2 Allele Causes Early-Onset Diabetes and Severe β-Cell Loss in
833 Munich Ins2C95S Mutant Mice. Diabetes. 2007 May 1;56(5):1268–76.

834 86. Tiano JP, Mauvais-Jarvis F. Importance of oestrogen receptors to preserve functional β-cell
835 mass in diabetes. Nat Rev Endocrinol. 2012 Jun;8(6):342–51.

836 87. Janson J, Soeller WC, Roche PC, Nelson RT, Torchia AJ, Kreutter DK, et al. Spontaneous
837 diabetes mellitus in transgenic mice expressing human islet amyloid polypeptide. Proc Natl Acad
838 Sci U S A. 1996 Jul 9;93(14):7283–8.

839 88. Walker EM, Cha J, Tong X, Guo M, Liu JH, Yu S, et al. Sex-biased islet β cell dysfunction is
840 caused by the MODY MAFA S64F variant by inducing premature aging and senescence in
841 males. Cell Rep. 2021 Oct 12;37(2):109813.

842 89. Mauvais-Jarvis F, Sobngwi E, Porcher R, Riveline JP, Kevorkian JP, Vaisse C, et al. Ketosis-
843 Prone Type 2 Diabetes in Patients of Sub-Saharan African Origin: Clinical Pathophysiology and
844 Natural History of β-Cell Dysfunction and Insulin Resistance. Diabetes. 2004 Mar 1;53(3):645–
845 53.

846 90. Iacovazzo D, Flanagan SE, Walker E, Quezado R, de Sousa Barros FA, Caswell R, et al. MAFA
847 missense mutation causes familial insulinomatosis and diabetes mellitus. Proc Natl Acad Sci U S
848 A. 2018 Jan 30;115(5):1027–32.

849 91. Xu B, Allard C, Alvarez-Mercado AI, Fuselier T, Kim JH, Coons LA, et al. Estrogens Promote
850 Misfolded Proinsulin Degradation to Protect Insulin Production and Delay Diabetes. Cell Rep.
851 2018 Jul 3;24(1):181.

852 92. Zhou Z, Ribas V, Rajbhandari P, Drew BG, Moore TM, Fluitt AH, et al. Estrogen receptor α
853 protects pancreatic β-cells from apoptosis by preserving mitochondrial function and suppressing
854 endoplasmic reticulum stress. J Biol Chem. 2018 Mar 30;293(13):4735.

855 93. Alonso-Magdalena P, Ropero AB, Carrera MP, Cederroth CR, Baquié M, Gauthier BR, et al.
856 Pancreatic insulin content regulation by the estrogen receptor ER alpha. PloS One. 2008 Apr
857 30;3(4):e2069.

858 94. Cnop M, Ladriere L, Hekerman P, Ortis F, Cardozo AK, Dogusan Z, et al. Selective Inhibition of
859 Eukaryotic Translation Initiation Factor 2α Dephosphorylation Potentiates Fatty Acid-induced
860 Endoplasmic Reticulum Stress and Causes Pancreatic β-Cell Dysfunction and Apoptosis *. J Biol
861 Chem. 2007 Feb 9;282(6):3989–97.

862 95. Oyadomari S, Koizumi A, Takeda K, Gotoh T, Akira S, Araki E, et al. Targeted disruption of the
863 Chop gene delays endoplasmic reticulum stress–mediated diabetes. J Clin Invest. 2002 Feb
864 15;109(4):525–32.

865 96. Han J, Back SH, Hur J, Lin YH, Gildersleeve R, Shan J, et al. ER-stress-induced transcriptional
866 regulation increases protein synthesis leading to cell death. Nat Cell Biol. 2013 May;15(5):481–
867 90.

868 97. Harding HP, Zeng H, Zhang Y, Jungries R, Chung P, Plesken H, et al. Diabetes Mellitus and
869 Exocrine Pancreatic Dysfunction in Perk−/− Mice Reveals a Role for Translational Control in
870 Secretory Cell Survival. Mol Cell. 2001 Jun 1;7(6):1153–63.

871 98. Novoa I, Zhang Y, Zeng H, Jungreis R, Harding HP, Ron D. Stress-induced gene expression
872 requires programmed recovery from translational repression. EMBO J. 2003 Mar 3;22(5):1180.

873 99. Ma Y, Hendershot LM. Delineation of a Negative Feedback Regulatory Loop That Controls
874 Protein Translation during Endoplasmic Reticulum Stress *. J Biol Chem. 2003 Sep
875 12;278(37):34864–73.

876 100. Panzhinskiy E, Skovsø S, Cen HH, Chu KY, MacDonald K, Soukhatcheva G, et al. Eukaryotic
877 translation initiation factor 2A protects pancreatic beta cells during endoplasmic reticulum stress
878 while rescuing translation inhibition. bioRxiv. 2021 Jan 1;2021.02.17.431676.

879 101. Cnop M, Toivonen S, Igoillo-Esteve M, Salpea P. Endoplasmic reticulum stress and eIF2α
880 phosphorylation: The Achilles heel of pancreatic β cells. Mol Metab. 2017 Jul 12;6(9):1024–39.

881 102. Marchetti P, Bugliani M, Lupi R, Marselli L, Masini M, Boggi U, et al. The endoplasmic reticulum
882 in pancreatic beta cells of type 2 diabetes patients. Diabetologia. 2007 Dec 1;50(12):2486–94.

883 103. Sharma RB, Darko C, Alonso LC. Intersection of the ATF6 and XBP1 ER stress pathways in
884 mouse islet cells. J Biol Chem. 2020 Oct 9;295(41):14164–77.

885 104. Nasteska D, Fine NHF, Ashford FB, Cuozzo F, Viloria K, Smith G, et al. PDX1LOW MAFALOW
886 β-cells contribute to islet function and insulin release. Nat Commun. 2021 Jan 29;12(1):674.

887 105. Talchai C, Xuan S, Lin HV, Sussel L, Accili D. Pancreatic β-Cell Dedifferentiation As Mechanism
888 Of Diabetic β-Cell Failure. Cell. 2012 Sep 14;150(6):1223.

889 106. Manicardi V, Russo G, Napoli A, Torlone E, Li Volsi P, Giorda CB, et al. Gender-Disparities in
890 Adults with Type 1 Diabetes: More Than a Quality of Care Issue. A Cross-Sectional
891 Observational Study from the AMD Annals Initiative. PLoS ONE. 2016 Oct 3;11(10):e0162960.

892
893
894 **FIGURE LEGENDS**

895 **Figure 1. Sex differences in human islet transcriptomic and functional responses in**
896 **type 2 diabetes.** scRNAseq data from male and female human β cells. For donor metadata
897 see Supplementary file 6. (A-C) Venn diagrams compare the number of significantly
898 differentially expressed genes between ND and T2D donors (*p*-adj<0.05). All differentially
899 expressed genes (A), downregulated genes (B), upregulated genes (C) in T2D human β cells.

900 For complete gene lists see Supplementary file 1. (D-F) Top 10 significantly enriched
901 Reactome pathways (ND vs T2D) from non-sex-specific (D), female (E), or male (F)
902 significantly differentially expressed genes (*p*-adj< 0.05). Gene ratio is calculated as *k/n*,
903 where *k* is the number of genes identified in each Reactome pathway, and *n* is the number of
904 genes from the submitted gene list participating in any Reactome pathway. For complete
905 Reactome pathway lists see Supplementary file 1. (G-K) Human islet perifusion data from the
906 Human Pancreas Analysis Program in ND and T2D donor islets in females (F, I) and males
907 (G, H). 3 mM glucose (3 mM G); 16.7 mM glucose (16.7 mM G); 0.1 mM
908 isobutylmethylxanthine (0.1 mM IBMX); 30 mM potassium chloride (30 mM KCl); 4 mM amino
909 acid mixture (4 mM AAM; mM: 0.44 alanine, 0.19 arginine, 0.038 aspartate, 0.094 citrulline,
910 0.12 glutamate, 0.30 glycine, 0.077 histidine, 0.094 isoleucine, 0.16 leucine, 0.37 lysine, 0.05
911 methionine, 0.70 ornithine, 0.08 phenylalanine, 0.35 proline, 0.57 serine, 0.27 threonine,
912 0.073 tryptophan, and 0.20 valine, 2 mM glutamine). (I-K) Quantification of area under the
913 curve (AUC) is shown for the various stimulatory media in females (I), males (J) and donors
914 with T2D (K). (I) In females, insulin secretion from ND islets was not significantly higher than
915 T2D islets. (J) In males, insulin secretion from ND islets was significantly higher than T2D
916 islets under 4 mM AAM +16.7 mM glucose (HG) + 0.1 mM IBMX stimulation (p=0.0442;
917 unpaired Student's *t*-test). (K) Total insulin secretion was lower in T2D male islets than ND
918 male islets (p=0.0503; unpaired Student's *t*-test). * indicates p<0.05; ns indicates not
919 significant; error bars indicate SEM.
920
921 **Figure 2. Sex-biased gene expression in mouse islet bulk RNAseq**. (A) Principal
922 component analysis (PCA) of RNAseq data from male and female mouse islets. (B) Over-
923 representation analysis (ORA) of all significantly differentially expressed genes (*p*-adj < 0.01)
924 from male and female mouse islets. Top 30 enriched KEGG pathways (large nodes; size =
925 proportional to connections, darker red color = greater significance) and associated genes
926 (small nodes; green = male enriched, yellow = female enriched). (C) Top significantly
927 enriched Reactome pathways from the top 1000 significantly differentially expressed genes.
928 (*p*-adj < 0.01) for males and females. Gene ratio is calculated as k/n, where k is the number of
929 genes identified in each Reactome pathway, and n is the number of genes from the submitted
930 gene list participating in any Reactome pathway. For complete Reactome pathway lists see
931 Supplementary file 1. (D) All transcripts of differentially expressed genes under the gene
932 ontology term "Cellular response to ER stress" (GO:0034976) and genes labeled by their role

933 in transcription, translation, protein processing, protein folding, secretion and protein quality
934 control. (E) All transcripts of differentially expressed ribosomal genes.
935
936 **Figure 3. Sex differences in mouse islet ER stress-associated phenotypes.** (A) Protein
937 synthesis was quantified in dispersed islet cells from 20-week-old male and female B6 mice
938 after treatment with 1 μM Tg for 2- or 24-hours. In female islet cells, protein synthesis was
939 significantly lower after a 2-hour Tg treatment compared to control (p=0.0152; paired
940 Student's *t*-test) and significantly higher after a 24-hour Tg treatment compared to a 2-hour Tg
941 treatment (p=0.0027; paired Student's *t*-test). In male islet cells, protein synthesis was
942 significantly lower after a 2- and 24-hour Tg treatment compared to control (p=0.0289 [0-2
943 hour] and p=0.0485 [0-24 hour]; paired Student's *t*-test). (B) In both male and female islet
944 cells protein synthesis was repressed after 2 hours. By 24 hours, protein synthesis repression
945 was resolved in female, but not male islet cells. (C-H) Quantification of propidium iodide (PI)
946 cell death assay of dispersed islets from 20-week-old male and female B6 mice treated with
947 thapsigargin (0.1 μM, 1 μM or 10 μM Tg) or DMSO for 84 hours. n=4-5 mice, >1000 cells per
948 group. Percentage (%) of PI positive cells was quantified as the number of PI-
949 positive/Hoechst 33342-positive cells in female (C) and male (D) islet cells. Relative cell death
950 at 84 hr in Tg treatments compared with DMSO treatment in females (E, G) and males (F, H).
951 In female islet cells, cell death was significantly higher in 10 μM Tg compared to control
952 (p<0.0001; unpaired Student's *t*-test). In male islet cells, cell death was significantly higher in
953 0.1, 1.0 and 10 μM Tg compared to control (p=0.0230 [0.1 μM], p<0.0001 [1 μM] and
954 p<0.0001 [10 μM]; unpaired Student's *t*-test) (D). For E-H, at 84 hours the % of PI positive
955 cells for each treatment was normalized to the DMSO control avg for each sex. * indicates
956 p<0.05, ** indicates p<0.01, **** indicates p<0.0001; ns indicates not significant; error bars
957 indicate SEM.
958
959 **Figure 4. Sex differences in *ex vivo* and *in vivo* insulin secretion**. (A) Experimental
960 workflow of static glucose-stimulated insulin secretion. (B, C) Relative high glucose (20 mM;
961 high glucose, HG) in treatments compared with DMSO in female (B) and male (C) islets.
962 Female islet HG secretion was significantly higher compared with control after 0- and 2-hour
963 Tg pre-treatments (p=0.0083 [0-hour] and p=0.0371 [2-hour]; Mann Whitney test). Male islet
964 HG secretion was significantly lower compared with control after a 4-hour Tg pre-treatment
965 (p=0.0013; Mann Whitney test). (D) Insulin content. Female islet insulin content was

966 significantly higher compared with control after a 4-hour Tg pre-treatment (p=0.0269; Mann
967 Whitney test). (E) Proinsulin content. Female islet proinsulin content was significantly lower
968 compared with control after a 2-hour Tg pre-treatment (p=0.0437; Mann Whitney test). Male
969 islet proinsulin content was significantly lower compared with control after 2- and 4-hour Tg
970 pre-treatments (p=0.0014 [2-hour] and p=0.0005 [4-hour]; Mann Whitney test). (F-H)
971 Physiology measurements after a 6-hour fast in 20-week-old male and female B6 mice. (F, G)
972 Insulin levels from glucose-stimulated insulin secretion tests (F: nM, G: % basal insulin)
973 following a single glucose injection (2 g glucose/kg body weight, i.p). Area under the curve
974 (AUC) calculations (n=13 females, n=18 males). (F) Insulin levels were significantly higher in
975 male mice at 0 minutes and 30 minutes post injection (p=0.0063 [0 minutes] and p=0.0009
976 [30 minutes]; Student's *t*-test). AUC was significantly higher in males (p=0.0159; Student's *t*-
977 test). (G) Insulin levels (% baseline). Glucose-stimulated insulin secretion was significantly
978 higher in female mice 15 minutes post injection (p=0.0279; Student's *t*-test). (H) Glucose
979 levels from glucose tolerance tests following a single glucose injection (2 g glucose/kg body
980 weight). AUC calculations (n=11 females, n=11 males). For B-E, grey triangles indicate the
981 concentration of insulin or proinsulin from five islets, black circles indicate the average values
982 per mouse. For B, ## indicates p<0.01 and ### indicates p<0.001 for comparisons between
983 treatments and DMSO in low glucose. For all other figures, * indicates p<0.05, ** indicates
984 p<0.01, *** indicates p<0.001; ns indicates not significant; error bars indicate SEM.
985
986 **Figure 5. Sex-specific transcriptomic and proteomic profiles following ER stress in**
987 **mouse islets.** (A) Principal component analysis (PCA) of RNAseq data from male and female
988 mouse islets treated with DMSO or 1 μM Tg for 6- or 12-hours. (B) Spearman correlation
989 depicting the variance for the first 5 principal components. (C) Top significantly enriched
990 Reactome pathways from the top 1000 significantly differentially expressed genes (*p*-
991 adj<0.01) for females and males that were upregulated or downregulated between 6-12 hours
992 of Tg treatment. Gene ratio is calculated as k/n, where k is the number of genes identified in
993 each Reactome pathway, and n is the number of genes from the submitted gene list
994 participating in any Reactome pathway. (D) Protein abundance from proteomics data of
995 female and male mouse islets treated with DMSO or 1 μM Tg for 6 hours. Top 45 differentially
996 expressed proteins are shown (p< 0.05).
997

998 **Table 1 – Human β cell pathway gene numbers.** The number of genes corresponding to
999 each T2D upregulated pathway in males, females or both sexes.
1000
1001 **SUPPLEMENTAL FIGURE LEGENDS**
1002 **Figure S1. Sex-specific and non-sex-specific differentially expressed genes in T2D.**
1003 scRNAseq data from male and female human β cells. (A-C) Top 60 significantly differentially
1004 expressed genes (*p*-adj < 0.05). Non-sex-specific (A), female-specific (B), or male-specific
1005 (C). For complete gene lists see Supplementary file 1.
1006
1007 **Figure S2. Gene expression changes in T2D.** scRNAseq data from male and female
1008 human β cells. (A, B) Top 60 differentially expressed genes (*p*-adj < 0.05) in females (A) and
1009 males (B). Sex-specific genes are indicated in red text. For complete gene lists see
1010 Supplementary file 1.
1011
1012 **Figure S3. Correlations between donor attributes and insulin secretion.** Pearson
1013 correlation of all human donors (A), or all donors with Type 2 Diabetes. Significant
1014 correlations are denoted with a star (*). For donor metadata see Supplementary file 6.
1015
1016 **Figure S4. Equivalent insulin sensitivity in male and female mice.** (A) Insulin tolerance
1017 test (ITT). 20-week-old female and male B6 mice were fasted for 6 hours. Glucose levels (%
1018 baseline) from insulin tolerance tests (ITT) following a single insulin injection (0.75U insulin/kg
1019 body weight). AUC calculations (n=11 females, n=11 males). ns indicates not significant; error
1020 bars indicate SEM.
1021
1022 **Figure S5. Mouse islet gene expression clusters by sex.** (A) Unsupervised hierarchical
1023 clustering of RNAseq data from female and male mouse islets. Sorting was based on all
1024 genes where the total count was >10 across all samples.
1025
1026 **Figure S6. ER stress-induced protein synthesis repression persists in male mouse islet**
1027 **cells.** (A) Representative images of dispersed islets stained with nuclear mask and OPP
1028 labeled with Alexa Fluor 594. (B, C) Integrated staining intensity of Alexa Fluor 594 in nuclear
1029 mask positive islet cells in control media (B, FBS+) or after treatment with DMSO control or 1
1030 μM Tg for 2- or 24-hours (C, FBS-). Protein synthesis is displayed on a per cell basis from

1031 data shown in Figure 3. n=4-5 mice, >1000 cells per group. Mean values are indicated under
1032 each group. (B) Protein synthesis was significantly higher in male islet cells than female islet
1033 cells in control media, 3.9% (p=0.027; unpaired Student's *t*-test). (C) In female islet cells,
1034 protein synthesis was significantly repressed from control-2 hour treatments (p=<0.0001;
1035 unpaired Student's *t*-test) and significantly increased from both control-24 hour treatments
1036 and 2-24 hour treatments (p=<0.0001; unpaired Student's *t*-test). In male islet cells, protein
1037 synthesis was significantly repressed from control-2 hour treatments (p=<0.0001; unpaired
1038 Student's *t*-test) and control-24 hour treatments (p=<0.0001; unpaired Student's *t*-test);
1039 however, was not significantly different between 2-24 hour treatments (p=0.07; unpaired
1040 Student's *t*-test). * indicates p<0.05, *** indicates p<0.001; ns indicates not significant; error
1041 bars indicate SEM.
1042
1043 **Figure S7. *Ins2* gene activity is repressed by ER stress induction.** *Ins2* gene activity in β
1044 cells from 20-week-old male and female B6 mice treated with Tg (0.1 μM or 1 μM Tg) or
1045 DMSO for 60 hours (n=6 mice per sex, > 1000 cells per group). (A, B) Average change in
1046 fluorescence intensity from all GFP expressing female (A) and male (B) β cells over time.
1047 Data was normalized to the first 2 hours to examine relative change in *Ins2* gene activity. (C,
1048 D) Density plot of *Ins2*$^{GFP/WT}$ β cell GFP fluorescence intensity, log transformed. Data is
1049 shown for each run for females (C) and males (D). (E-H) Average change in high (E, F) and
1050 low (G,H) GFP *Ins2*$^{GFP/WT}$ β cells fluorescence over time from females (E, G) and males (F,
1051 H). Data was normalized to the first two hours to examine relative change in *Ins2* gene
1052 activity.
1053
1054 **Figure S8. Representative western blot images of UPR protein markers.** (A-D) Levels of
1055 ER stress proteins were quantified in isolated islets from 20-week-old male and female B6
1056 mice cultured in DMSO or 1 μM Tg for 24 hours. (A) BiP levels were significantly upregulated
1057 in female Tg vs DMSO (p=0.0011; paired Student's *t*-test) but not male Tg vs DMSO
1058 (p=0.1187; paired Student's *t*-test). (B) pIRE1α levels were significantly upregulated in female
1059 Tg vs DMSO (p=0.0001; paired Student's *t*-test) and in male Tg vs DMSO (p=0.0148; paired
1060 Student's *t*-test). (C) CHOP levels were significantly upregulated in female Tg vs DMSO
1061 (p=0.0333; paired Student's *t*-test) and in male Tg vs DMSO (p=0.0164; paired Student's *t*-
1062 test). (D) p-eIF2α levels were not significantly upregulated in either sex. (E-G) Levels of ER
1063 stress proteins were quantified in isolated islets from 60-week-old male and female B6 mice

1064 cultured in DMSO or 1 μM Tg for 24 hours. (E) BiP levels were significantly upregulated in
1065 male Tg vs DMSO (p=0.0048; paired Student's *t*-test) but not in female Tg vs DMSO
1066 (p=0.3319; paired Student's *t*-test). (F) p-IRE1α levels were not significantly upregulated in
1067 either sex (p=0.9257 [female] and p=0.8273 [male]; paired Student's *t*-test). (G) p-eIF2α
1068 levels were not significantly upregulated in either sex (p=0.8451 [female] and p=0.3076
1069 [male]; paired Student's *t*-test). (H) Representative western blot images of 20-week Tg treated
1070 mouse islets. (I) Representative western blot images of 60-week Tg treated mouse islets. *
1071 indicates p<0.05, ** indicates p<0.01; ns indicates not significant.
1072
1073 **Figure S9. Female mouse islets retain greater insulin secretion during ER stress.** (A)
1074 Insulin secretion at basal (3 mM; low glucose, LG) and stimulatory (20 mM; high glucose, HG)
1075 glucose. Female islet LG secretion was significantly higher compared with control after 2- and
1076 4-hour Tg pre-treatments (p=0.0047 [2-hour] and p=0.0003 [4-hour]; Mann Whitney test).
1077 Female islet HG secretion was significantly higher compared with control after 0- and 2-hour
1078 Tg pre-treatments (p=0.0012 [0-hour] and p=0.0061 [2-hour]; Mann Whitney test). Male islet
1079 LG secretion was significantly higher compared with control after a 0-hour Tg pre-treatment
1080 (p=0.0371; Mann Whitney test). Male islet HG secretion was significantly lower compared with
1081 control after a 4-hour Tg pre-treatment (p=0.0012; Mann Whitney test). (B) Proinsulin
1082 secretion at basal (3 mM) and stimulatory (20 mM) glucose. Female islet HG secretion was
1083 significantly higher compared with control after 0- and 2-hour Tg pre-treatments (p=0.0075 [0-
1084 hour] and p=0.0437 [2-hour],; Mann Whitney test). Male islet HG secretion was significantly
1085 lower compared with control after a 4-hour Tg pre-treatment (p=0.0025; Mann Whitney test). *
1086 indicates p<0.05, ** indicates p<0.01; ns indicates not significant; error bars indicate SEM.
1087
1088 **Figure S10. Mouse islet gene expression clusters by sex, treatment and time.** (A)
1089 Unsupervised hierarchical clustering of RNAseq data from female and male DMSO or Tg
1090 treated mouse islets. Sorting was based on all genes where the total count >10 across all
1091 samples.
1092
1093 **Figure S11. Female and Male mouse islets are enriched in similar pathways following**
1094 **6- and 12-hour Tg treatments.** (A, B) Most significantly enriched Reactome pathways from
1095 the top 1000 significantly differentially expressed genes. (*p*-adj < 0.01) for females and males
1096 between DMSO vs Tg after 6 hours (A) or 12 hours (B) of Tg treatment. Gene ratio is

1097 calculated as k/n, where k is the number of genes identified in each Reactome pathway, and
1098 n is the number of genes from the submitted gene list participating in any Reactome pathway.
1099
1100 **Figure S12. A greater number of β cell identity genes are downregulated between 6-**
1101 **and 12- hour Tg treatment times in female mouse islets.** (A, B) Treatment:Time interaction
1102 plots of female islet (A) and male islet (B) β cell identity genes in Reactome pathway
1103 "Regulation of gene expression in β cells". The fold change (FC) for DMSO vs Tg was
1104 calculated for each sex and time point (Female 6-hour, Female 12-hour, Male 6-hour, Male
1105 12-hour). The change in FC values (12-hour FC – 6-hour FC) were plotted according to *p*-adj
1106 values. In females, FC values between 6- and 12-hours are represented by orange and
1107 purple dots, respectively. In males, FC values at 6- and 12-hours are represented by green
1108 and blue dots, respectively. A solid black line connecting the dots indicates genes with a
1109 significant treatment:time interaction.

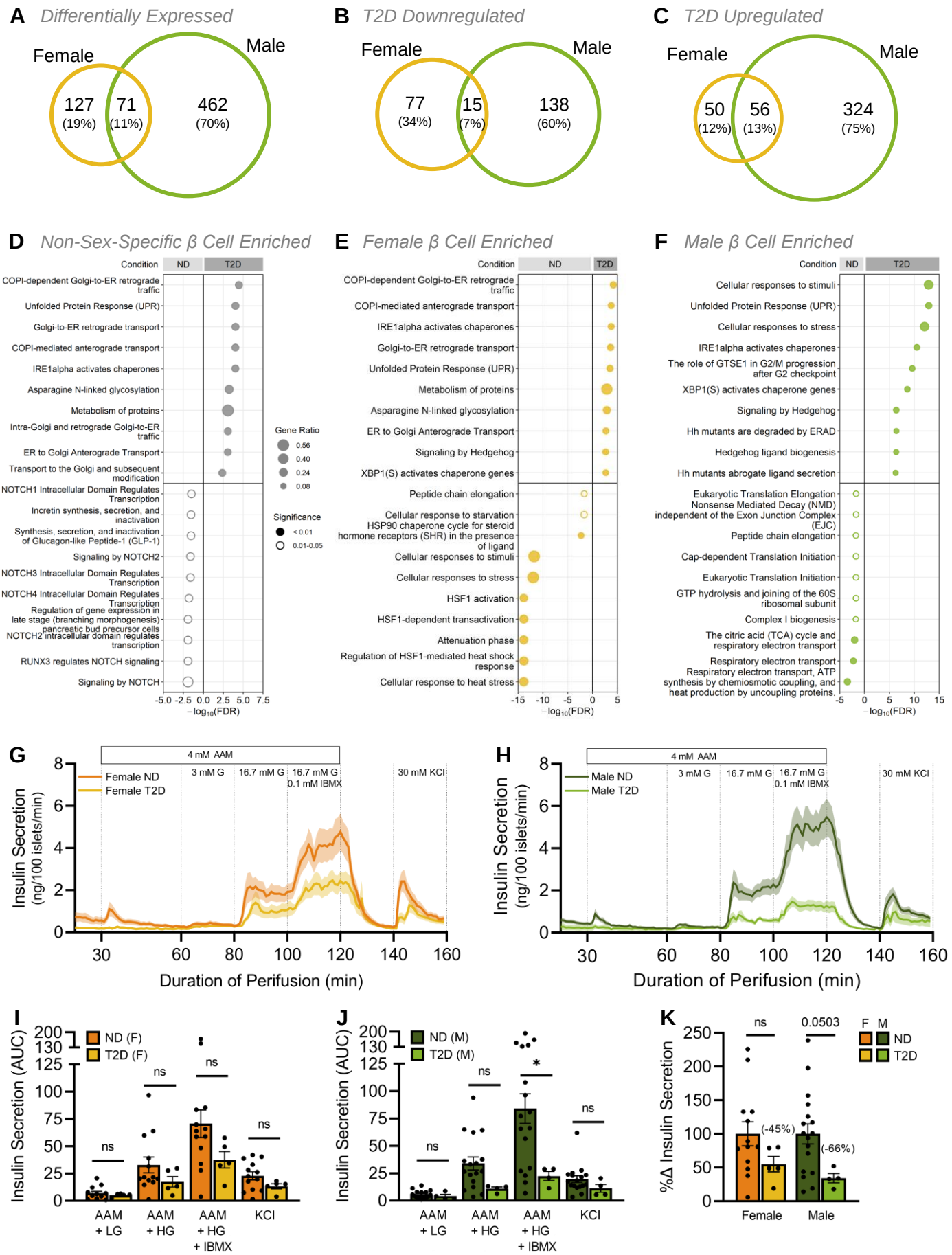
A Differentially Expressed
Female
Male
127 (19%)
71 (11%)
462 (70%)
B T2D Downregulated
Female
Male
77 (34%)
15 (7%)
138 (60%)
C T2D Upregulated
Female
Male
50 (12%)
56 (13%)
324 (75%)
D Non-Sex-Specific β Cell Enriched
Condition
ND
T2D
COPI-dependent Golgi-to-ER retrograde traffic
Unfolded Protein Response (UPR)
Golgi-to-ER retrograde transport
COPI-mediated anterograde transport
IRE1alpha activates chaperones
Asparagine N-linked glycosylation
Metabolism of proteins
Intra-Golgi and retrograde Golgi-to-ER traffic
ER to Golgi Anterograde Transport
Transport to the Golgi and subsequent modification
NOTCH1 Intracellular Domain Regulates Transcription
Incretin synthesis, secretion, and inactivation
Synthesis, secretion, and inactivation of Glucagon-like Peptide-1 (GLP-1)
Signaling by NOTCH2
NOTCH3 Intracellular Domain Regulates Transcription
NOTCH4 Intracellular Domain Regulates Transcription
Regulation of gene expression in late stage (branching morphogenesis) pancreatic bud precursor cells
NOTCH2 intracellular domain regulates transcription
RUNX3 regulates NOTCH signaling
Signaling by NOTCH
Gene Ratio
0.56
0.40
0.24
0.08
Significance
< 0.01
0.01-0.05
-5.0 -2.5 0.0 2.5 5.0 7.5
−log10(FDR)
E Female β Cell Enriched
Condition
ND
T2D
COPI-dependent Golgi-to-ER retrograde traffic
COPI-mediated anterograde transport
IRE1alpha activates chaperones
Golgi-to-ER retrograde transport
Unfolded Protein Response (UPR)
Metabolism of proteins
Asparagine N-linked glycosylation
ER to Golgi Anterograde Transport
Signaling by Hedgehog
XBP1(S) activates chaperone genes
Peptide chain elongation
Cellular response to starvation
HSP90 chaperone cycle for steroid hormone receptors (SHR) in the presence of ligand
Cellular responses to stimuli
Cellular responses to stress
HSF1 activation
HSF1-dependent transactivation
Attenuation phase
Regulation of HSF1-mediated heat shock response
Cellular response to heat stress
-15 -10 -5 0 5
−log10(FDR)
F Male β Cell Enriched
Condition
ND
T2D
Cellular responses to stimuli
Unfolded Protein Response (UPR)
Cellular responses to stress
IRE1alpha activates chaperones
The role of GTSE1 in G2/M progression after G2 checkpoint
XBP1(S) activates chaperone genes
Signaling by Hedgehog
Hh mutants are degraded by ERAD
Hedgehog ligand biogenesis
Hh mutants abrogate ligand secretion
Eukaryotic Translation Elongation
Nonsense Mediated Decay (NMD) independent of the Exon Junction Complex (EJC)
Peptide chain elongation
Cap-dependent Translation Initiation
Eukaryotic Translation Initiation
GTP hydrolysis and joining of the 60S ribosomal subunit
Complex I biogenesis
The citric acid (TCA) cycle and respiratory electron transport
Respiratory electron transport
Respiratory electron transport, ATP synthesis by chemiosmotic coupling, and heat production by uncoupling proteins.
-5 0 5 10 15
−log10(FDR)
G
4 mM AAM
3 mM G
16.7 mM G
16.7 mM G 0.1 mM IBMX
30 mM KCl
Female ND
Female T2D
Insulin Secretion (ng/100 islets/min)
0 2 4 6 8
30 60 80 100 120 140 160
Duration of Perifusion (min)
H
4 mM AAM
3 mM G
16.7 mM G
16.7 mM G 0.1 mM IBMX
30 mM KCl
Male ND
Male T2D
Insulin Secretion (ng/100 islets/min)
0 2 4 6 8
30 60 80 100 120 140 160
Duration of Perifusion (min)
I
ND (F)
T2D (F)
Insulin Secretion (AUC)
0 25 50 75 100 125 130 200
ns
ns
ns
ns
AAM + LG
AAM + HG
AAM + HG + IBMX
KCl
J
ND (M)
T2D (M)
Insulin Secretion (AUC)
0 25 50 75 100 125 130 200
ns
ns
*
ns
AAM + LG
AAM + HG
AAM + HG + IBMX
KCl
K
ns
0.0503
F M
ND
T2D
%Δ Insulin Secretion
0 50 100 150 200 250
(-45%)
(-66%)
Female
Male

Figure 1

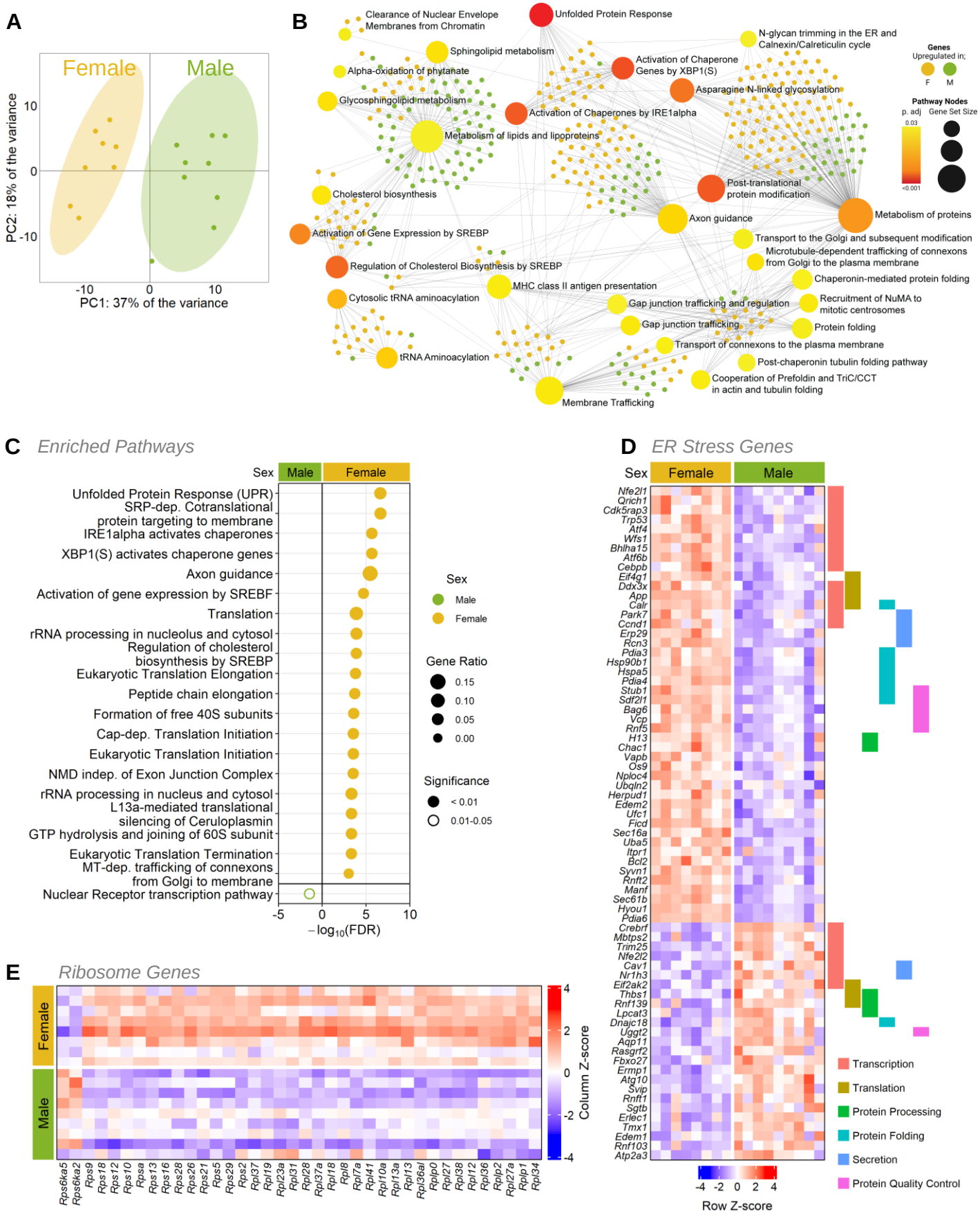
A
Female
Male
PC2: 18% of the variance
PC1: 37% of the variance
10
0
-10
B
Clearance of Nuclear Envelope Membranes from Chromatin
Unfolded Protein Response
N-glycan trimming in the ER and Calnexin/Calreticulin cycle
Sphingolipid metabolism
Alpha-oxidation of phytanate
Activation of Chaperone Genes by XBP1(S)
Asparagine N-linked glycosylation
Glycosphingolipid metabolism
Activation of Chaperones by IRE1alpha
Metabolism of lipids and lipoproteins
Cholesterol biosynthesis
Post-translational protein modification
Axon guidance
Metabolism of proteins
Activation of Gene Expression by SREBP
Transport to the Golgi and subsequent modification
Microtubule-dependent trafficking of connexons from Golgi to the plasma membrane
Regulation of Cholesterol Biosynthesis by SREBP
Chaperonin-mediated protein folding
MHC class II antigen presentation
Cytosolic tRNA aminoacylation
Gap junction trafficking and regulation
Recruitment of NuMA to mitotic centrosomes
Gap junction trafficking
Protein folding
Transport of connexons to the plasma membrane
tRNA Aminoacylation
Post-chaperonin tubulin folding pathway
Cooperation of Prefoldin and TriC/CCT in actin and tubulin folding
Membrane Trafficking
Genes
Upregulated in;
F
M
Pathway Nodes
p. adj
Gene Set Size
0.03
<0.001
C
Enriched Pathways
Sex
Male
Female
Unfolded Protein Response (UPR)
SRP-dep. Cotranslational protein targeting to membrane
IRE1alpha activates chaperones
XBP1(S) activates chaperone genes
Axon guidance
Activation of gene expression by SREBF
Translation
rRNA processing in nucleolus and cytosol
Regulation of cholesterol biosynthesis by SREBP
Eukaryotic Translation Elongation
Peptide chain elongation
Formation of free 40S subunits
Cap-dep. Translation Initiation
Eukaryotic Translation Initiation
NMD indep. of Exon Junction Complex
rRNA processing in nucleus and cytosol
L13a-mediated translational silencing of Ceruloplasmin
GTP hydrolysis and joining of 60S subunit
Eukaryotic Translation Termination
MT-dep. trafficking of connexons from Golgi to membrane
Nuclear Receptor transcription pathway
-5
0
5
10
−log10(FDR)
Sex
Male
Female
Gene Ratio
0.15
0.10
0.05
0.00
Significance
< 0.01
0.01-0.05
D
ER Stress Genes
Sex
Female
Male
Nfe2l1
Qrich1
Cdk5rap3
Trp53
Atf4
Wfs1
Bhlha15
Atf6b
Cebpb
Eif4g1
Ddx3x
App
Calr
Park7
Ccnd1
Erp29
Rcn3
Pdia3
Hsp90b1
Hspa5
Pdia4
Stub1
Sdf2l1
Bag6
Vcp
Rnf5
H13
Chac1
Vapb
Os9
Nploc4
Ubqln2
Herpud1
Edem2
Ufc1
Ficd
Sec16a
Uba5
Itpr1
Bcl2
Syvn1
Rnft2
Manf
Sec61b
Hyou1
Pdia6
Crebrf
Mbtps2
Trim25
Nfe2l2
Cav1
Nr1h3
Eif2ak2
Thbs1
Rnf139
Lpcat3
Dnajc18
Uggt2
Aqp11
Rasgrf2
Fbxo27
Ermp1
Atg10
Svip
Rnft1
Sgtb
Erlec1
Tmx1
Edem1
Rnf103
Atp2a3
Transcription
Translation
Protein Processing
Protein Folding
Secretion
Protein Quality Control
-4
-2
0
2
4
Row Z-score
E
Ribosome Genes
Female
Male
Rps6ka5
Rps6ka2
Rps9
Rps18
Rps12
Rps10
Rpsa
Rps13
Rps16
Rps28
Rps26
Rps21
Rps5
Rps29
Rps2
Rpl37
Rpl19
Rpl23a
Rpl31
Rpl28
Rpl37a
Rpl18
Rpl8
Rpl7a
Rpl41
Rpl10a
Rpl13a
Rpl13
Rpl36al
Rplp0
Rpl27
Rpl38
Rpl12
Rpl36
Rplp2
Rpl27a
Rplp1
Rpl34
4
2
0
-2
-4
Column Z-score

Figure 2

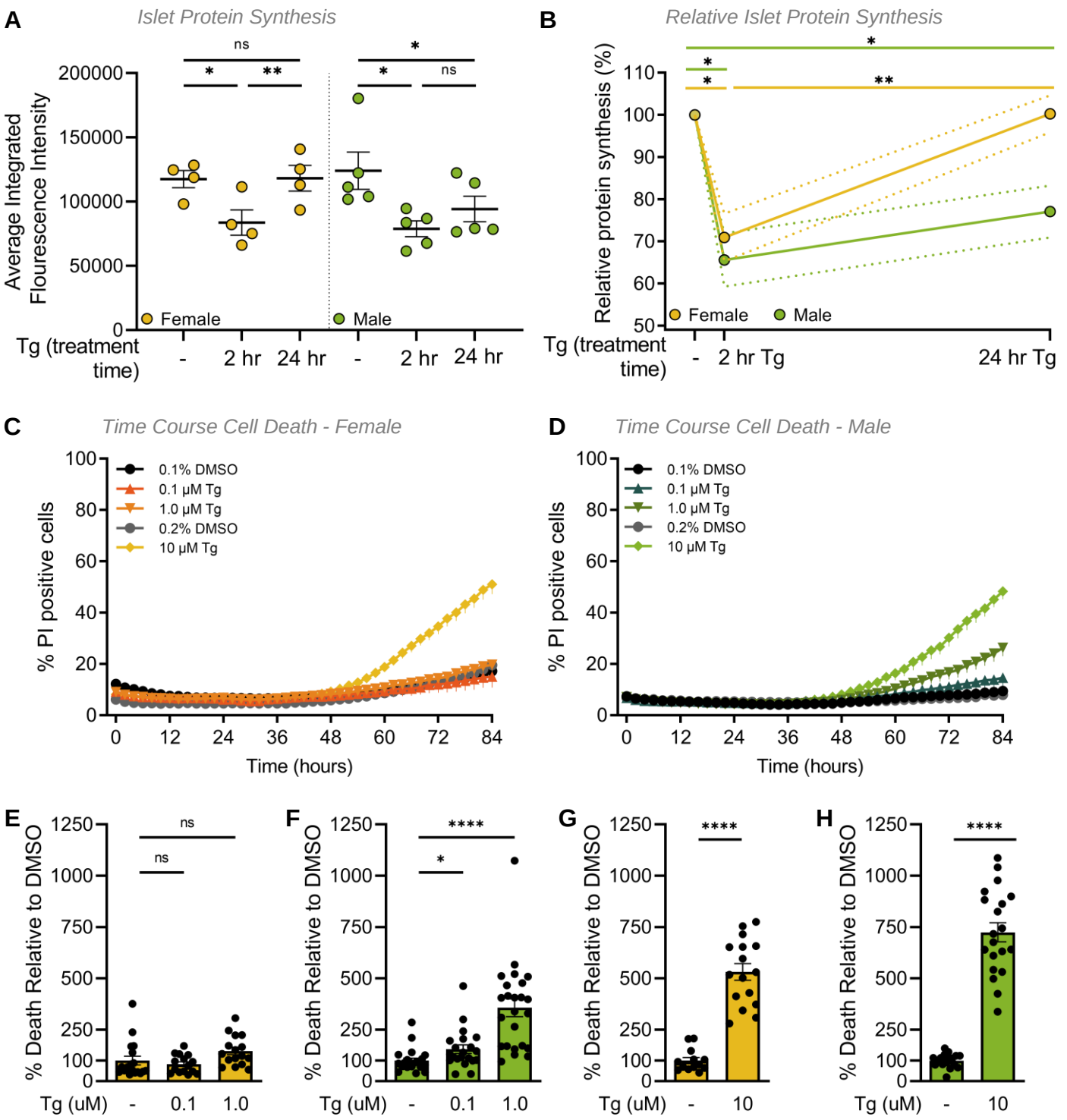
A
Islet Protein Synthesis
Average Integrated Flourescence Intensity
200000
150000
100000
50000
0
ns
*
**
*
*
ns
Female
Male
Tg (treatment time)
-
2 hr
24 hr
-
2 hr
24 hr
B
Relative Islet Protein Synthesis
Relative protein synthesis (%)
110
100
90
80
70
60
50
*
*
*
**
Female
Male
Tg (treatment time)
-
2 hr Tg
24 hr Tg
C
Time Course Cell Death - Female
% PI positive cells
0.1% DMSO
0.1 μM Tg
1.0 μM Tg
0.2% DMSO
10 μM Tg
Time (hours)
D
Time Course Cell Death - Male
% PI positive cells
0.1% DMSO
0.1 μM Tg
1.0 μM Tg
0.2% DMSO
10 μM Tg
Time (hours)
E
% Death Relative to DMSO
ns
ns
Tg (uM)
-
0.1
1.0
F
% Death Relative to DMSO
****
*
Tg (uM)
-
0.1
1.0
G
% Death Relative to DMSO
****
Tg (uM)
-
10
H
% Death Relative to DMSO
****
Tg (uM)
-
10

Figure 3

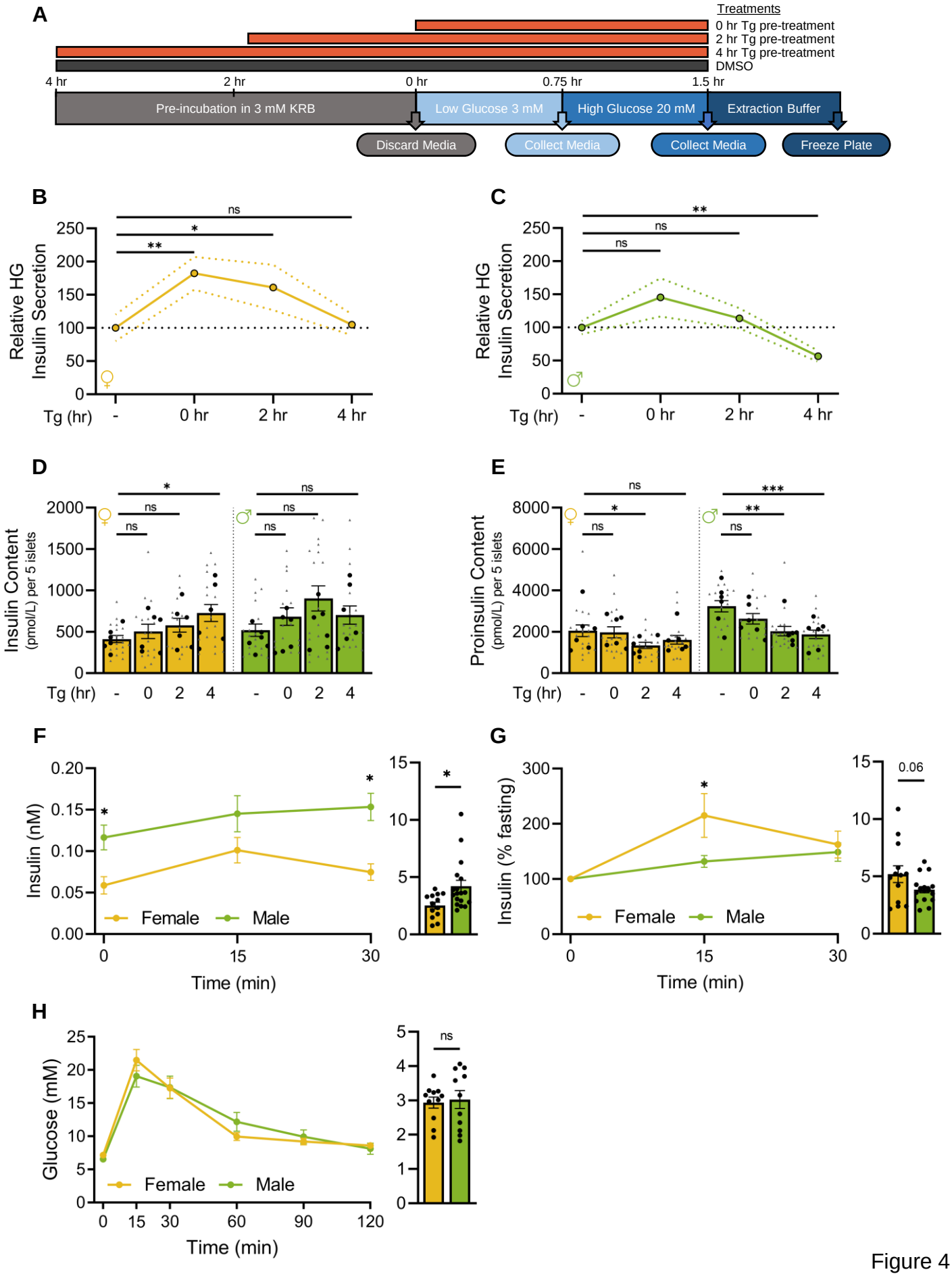
A
Treatments
0 hr Tg pre-treatment
2 hr Tg pre-treatment
4 hr Tg pre-treatment
DMSO
4 hr
2 hr
0 hr
0.75 hr
1.5 hr
Pre-incubation in 3 mM KRB
Low Glucose 3 mM
High Glucose 20 mM
Extraction Buffer
Discard Media
Collect Media
Collect Media
Freeze Plate
B
Relative HG Insulin Secretion
Tg (hr)
C
Relative HG Insulin Secretion
Tg (hr)
D
Insulin Content (pmol/L) per 5 islets
Tg (hr)
E
Proinsulin Content (pmol/L) per 5 islets
Tg (hr)
F
Insulin (nM)
Time (min)
Female
Male
G
Insulin (% fasting)
Time (min)
Female
Male
H
Glucose (mM)
Time (min)
Female
Male

Figure 4

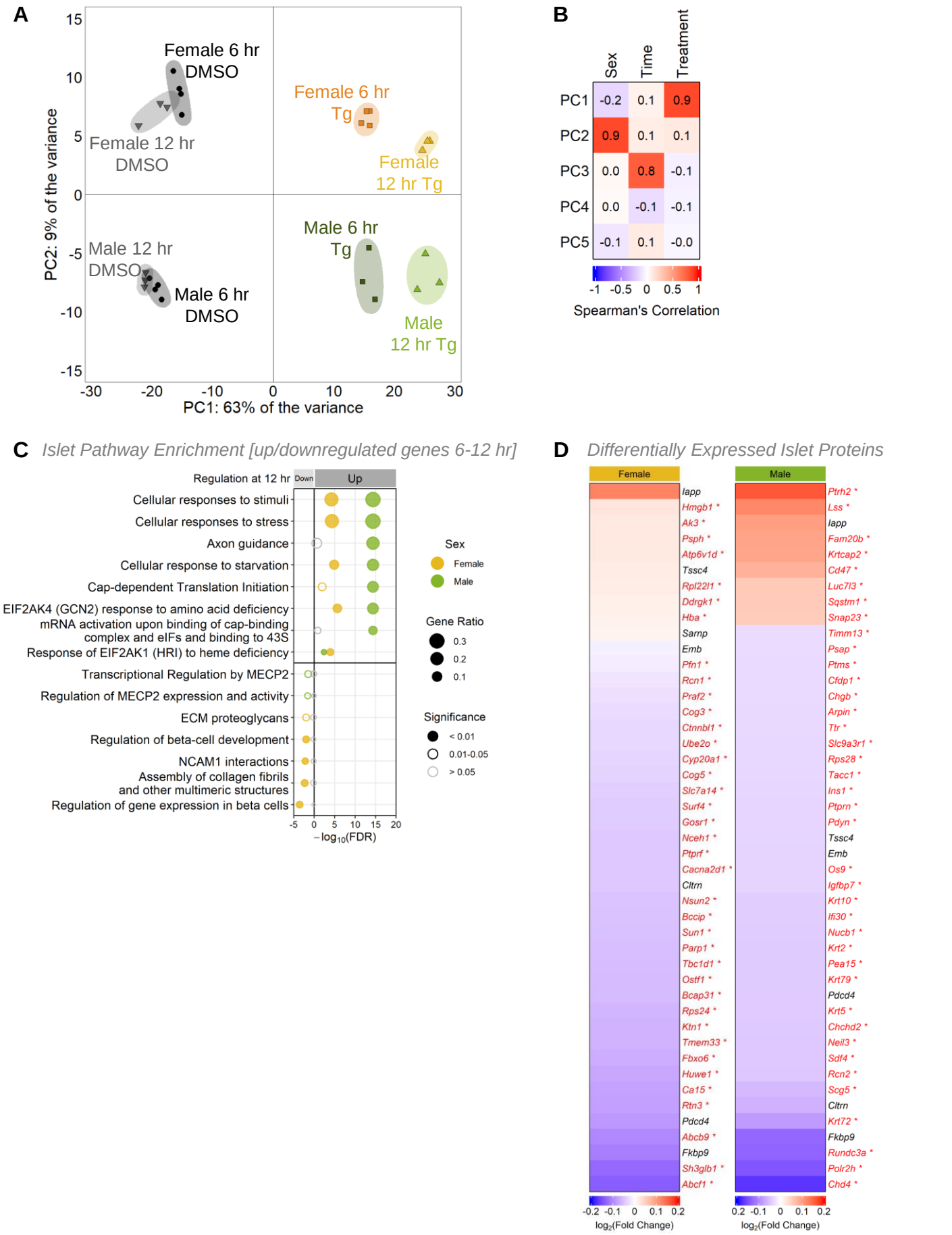
A
Female 6 hr DMSO
Female 12 hr DMSO
Female 6 hr Tg
Female 12 hr Tg
Male 12 hr DMSO
Male 6 hr DMSO
Male 6 hr Tg
Male 12 hr Tg
PC2: 9% of the variance
PC1: 63% of the variance
B
Sex
Time
Treatment
PC1 -0.2 0.1 0.9
PC2 0.9 0.1 0.1
PC3 0.0 0.8 -0.1
PC4 0.0 -0.1 -0.1
PC5 -0.1 0.1 -0.0
Spearman's Correlation
C Islet Pathway Enrichment [up/downregulated genes 6-12 hr]
Regulation at 12 hr
Down
Up
Cellular responses to stimuli
Cellular responses to stress
Axon guidance
Cellular response to starvation
Cap-dependent Translation Initiation
EIF2AK4 (GCN2) response to amino acid deficiency
mRNA activation upon binding of cap-binding complex and eIFs and binding to 43S
Response of EIF2AK1 (HRI) to heme deficiency
Transcriptional Regulation by MECP2
Regulation of MECP2 expression and activity
ECM proteoglycans
Regulation of beta-cell development
NCAM1 interactions
Assembly of collagen fibrils and other multimeric structures
Regulation of gene expression in beta cells
−log10(FDR)
Sex
Female
Male
Gene Ratio
0.3
0.2
0.1
Significance
< 0.01
0.01-0.05
> 0.05
D Differentially Expressed Islet Proteins
Female
Male
Iapp
Hmgb1 *
Ak3 *
Psph *
Atp6v1d *
Tssc4
Rpl22l1 *
Ddrgk1 *
Hba *
Sarnp
Emb
Pfn1 *
Rcn1 *
Praf2 *
Cog3 *
Ctnnbl1 *
Ube2o *
Cyp20a1 *
Cog5 *
Slc7a14 *
Surf4 *
Gosr1 *
Nceh1 *
Ptprf *
Cacna2d1 *
Cltrn
Nsun2 *
Bccip *
Sun1 *
Parp1 *
Tbc1d1 *
Ostf1 *
Bcap31 *
Rps24 *
Ktn1 *
Tmem33 *
Fbxo6 *
Huwe1 *
Ca15 *
Rtn3 *
Pdcd4
Abcb9 *
Fkbp9
Sh3glb1 *
Abcf1 *
Ptrh2 *
Lss *
Iapp
Fam20b *
Krtcap2 *
Cd47 *
Luc7l3 *
Sqstm1 *
Snap23 *
Timm13 *
Psap *
Ptms *
Cfdp1 *
Chgb *
Arpin *
Ttr *
Slc9a3r1 *
Rps28 *
Tacc1 *
Ins1 *
Ptprn *
Pdyn *
Tssc4
Emb
Os9 *
Igfbp7 *
Krt10 *
Ifi30 *
Nucb1 *
Krt2 *
Pea15 *
Krt79 *
Pdcd4
Krt5 *
Chchd2 *
Neil3 *
Sdf4 *
Rcn2 *
Scg5 *
Cltrn
Krt72 *
Fkbp9
Rundc3a *
Polr2h *
Chd4 *
log2(Fold Change)
log2(Fold Change)

Figure 5

	Number of Pathway Genes		
Pathway Name	Unique Male	Common	Unique Female
Asparagine N-linked glycosylation	16	9	4
Cellular responses to stimuli	49	9	6
Cellular responses to stress	47	9	6
COPI-dependent Golgi-to-ER retrograde traffic	7	6	2
COPI-mediated anterograde transport	7	5	2
ER to Golgi Anterograde Transport	10	5	2
Golgi-to-ER retrograde transport	7	6	2
Hedgehog ligand biogenesis	12	4	1
Hh mutants abrogate ligand secretion	12	3	1
Hh mutants are degraded by ERAD	12	3	1
IRE1alpha activates chaperones	9	3	1
Metabolism of proteins	69	20	13
Signaling by Hedgehog	16	6	2
The role of GTSE1 in G2/M progression after G2 checkpoint	14	4	1
Unfolded Protein Response (UPR)	13	3	1
XBP1(S) activates chaperone genes	8	3	1

Table 1

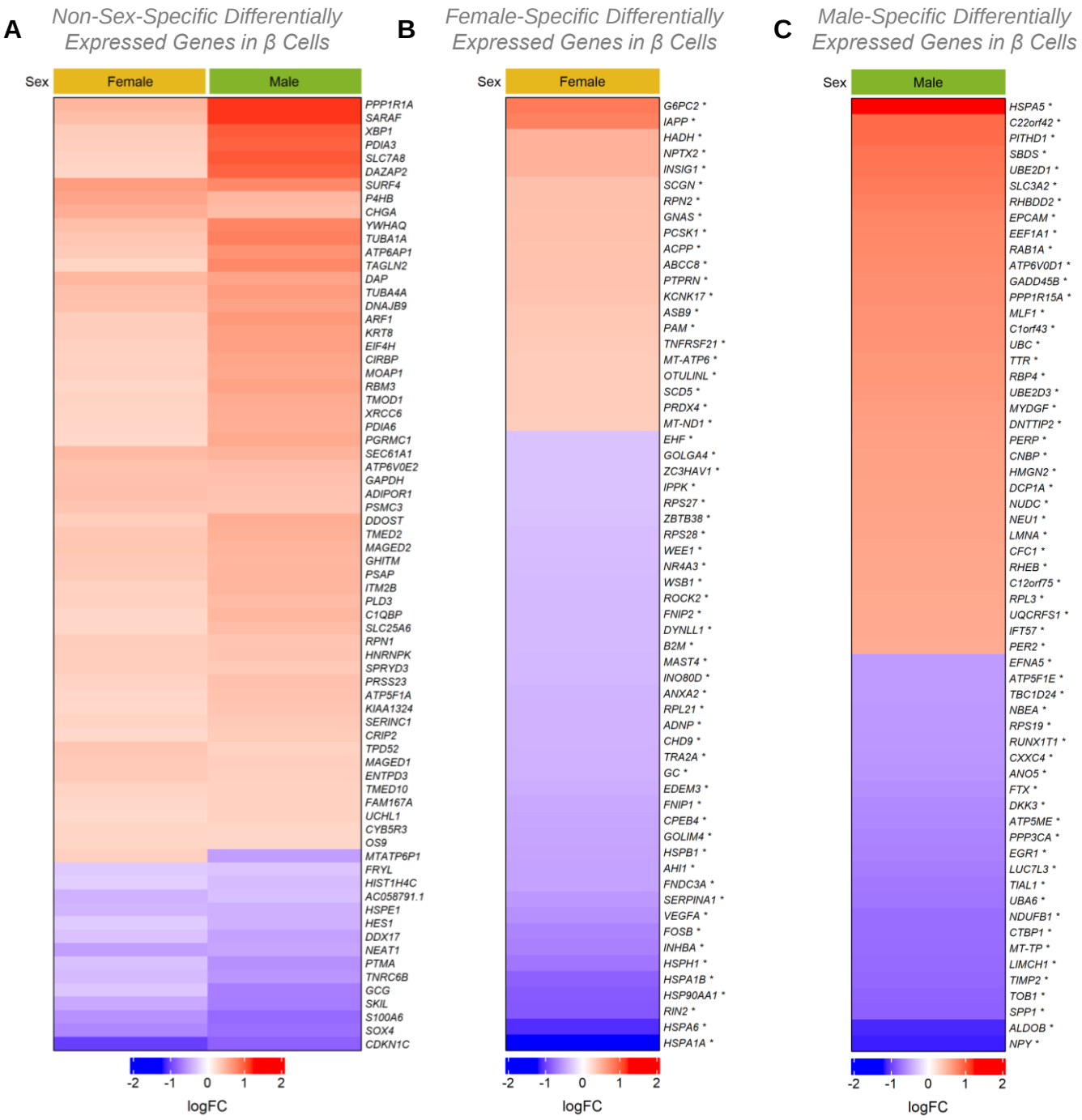
A
Non-Sex-Specific Differentially Expressed Genes in β Cells
Sex
Female
Male
PPP1R1A
SARAF
XBP1
PDIA3
SLC7A8
DAZAP2
SURF4
P4HB
CHGA
YWHAQ
TUBA1A
ATP6AP1
TAGLN2
DAP
TUBA4A
DNAJB9
ARF1
KRT8
EIF4H
CIRBP
MOAP1
RBM3
TMOD1
XRCC6
PDIA6
PGRMC1
SEC61A1
ATP6V0E2
GAPDH
ADIPOR1
PSMC3
DDOST
TMED2
MAGED2
GHITM
PSAP
ITM2B
PLD3
C1QBP
SLC25A6
RPN1
HNRNPK
SPRYD3
PRSS23
ATP5F1A
KIAA1324
SERINC1
CRIP2
TPD52
MAGED1
ENTPD3
TMED10
FAM167A
UCHL1
CYB5R3
OS9
MTATP6P1
FRYL
HIST1H4C
AC058791.1
HSPE1
HES1
DDX17
NEAT1
PTMA
TNRC6B
GCG
SKIL
S100A6
SOX4
CDKN1C
-2 -1 0 1 2
logFC
B
Female-Specific Differentially Expressed Genes in β Cells
Sex
Female
G6PC2 *
IAPP *
HADH *
NPTX2 *
INSIG1 *
SCGN *
RPN2 *
GNAS *
PCSK1 *
ACPP *
ABCC8 *
PTPRN *
KCNK17 *
ASB9 *
PAM *
TNFRSF21 *
MT-ATP6 *
OTULINL *
SCD5 *
PRDX4 *
MT-ND1 *
EHF *
GOLGA4 *
ZC3HAV1 *
IPPK *
RPS27 *
ZBTB38 *
RPS28 *
WEE1 *
NR4A3 *
WSB1 *
ROCK2 *
FNIP2 *
DYNLL1 *
B2M *
MAST4 *
INO80D *
ANXA2 *
RPL21 *
ADNP *
CHD9 *
TRA2A *
GC *
EDEM3 *
FNIP1 *
CPEB4 *
GOLIM4 *
HSPB1 *
AHI1 *
FNDC3A *
SERPINA1 *
VEGFA *
FOSB *
INHBA *
HSPH1 *
HSPA1B *
HSP90AA1 *
RIN2 *
HSPA6 *
HSPA1A *
-2 -1 0 1 2
logFC
C
Male-Specific Differentially Expressed Genes in β Cells
Sex
Male
HSPA5 *
C22orf42 *
PITHD1 *
SBDS *
UBE2D1 *
SLC3A2 *
RHBDD2 *
EPCAM *
EEF1A1 *
RAB1A *
ATP6V0D1 *
GADD45B *
PPP1R15A *
MLF1 *
C1orf43 *
UBC *
TTR *
RBP4 *
UBE2D3 *
MYDGF *
DNTTIP2 *
PERP *
CNBP *
HMGN2 *
DCP1A *
NUDC *
NEU1 *
LMNA *
CFC1 *
RHEB *
C12orf75 *
RPL3 *
UQCRFS1 *
IFT57 *
PER2 *
EFNA5 *
ATP5F1E *
TBC1D24 *
NBEA *
RPS19 *
RUNX1T1 *
CXXC4 *
ANO5 *
FTX *
DKK3 *
ATP5ME *
PPP3CA *
EGR1 *
LUC7L3 *
TIAL1 *
UBA6 *
NDUFB1 *
CTBP1 *
MT-TP *
LIMCH1 *
TIMP2 *
TOB1 *
SPP1 *
ALDOB *
NPY *
-2 -1 0 1 2
logFC

Figure S1

A
Top 60 Differentially Expressed Genes in Female β Cells
Sex
Female
G6PC2 *
IAPP *
SURF4
P4HB
CHGA
HADH *
NPTX2 *
INSIG1 *
PPP1R1A
DAP
SEC61A1
SARAF
YWHAQ
SCGN *
TUBA4A
RPN2 *
ADIPOR1
DNAJB9
GNAS *
PCSK1 *
GAPDH
ACPP *
ATP6V0E2
ABCC8 *
PTPRN *
KCNK17 *
PSMC3
B2M *
MAST4 *
INO80D *
HSPE1
ANXA2 *
RPL21 *
ADNP *
CHD9 *
TRA2A *
GC *
AC058791.1
EDEM3 *
SKIL
FNIP1 *
CPEB4 *
GOLIM4 *
HSPB1 *
AHI1 *
FNDC3A *
NEAT1
SERPINA1 *
S100A6
VEGFA *
SOX4
FOSB *
INHBA *
HSPH1 *
HSPA1B *
HSP90AA1 *
RIN2 *
CDKN1C
HSPA6 *
HSPA1A *
-2 -1 0 1 2
logFC
*Indicates genes unique to females
B
Top 60 Differentially Expressed Genes in Male β Cells
Sex
Male
HSPA5 *
SARAF
PPP1R1A
SLC7A8
XBP1
PDIA3
DAZAP2
C22orf42 *
PITHD1 *
SBDS *
UBE2D1 *
SLC3A2 *
TUBA1A
RHBDD2 *
YWHAQ
EPCAM *
TAGLN2
SURF4
EEF1A1 *
RAB1A *
ATP6V0D1 *
GADD45B *
PPP1R15A *
ATP6AP1
MLF1 *
C1orf43 *
UBC *
TTR *
RBP4 *
UBE2D3 *
ARF1
TUBA4A
MYDGF *
DNTTIP2 *
PERP *
EIF4H
KRT8
CNBP *
FTX *
DKK3 *
ATP5ME *
PPP3CA *
EGR1 *
GCG
SKIL
LUC7L3 *
TIAL1 *
UBA6 *
SOX4
NDUFB1 *
CTBP1 *
MT-TP *
S100A6
LIMCH1 *
TIMP2 *
TOB1 *
CDKN1C
SPP1 *
ALDOB *
NPY *
-2 -1 0 1 2
logFC
*Indicates genes unique to males

Figure S2

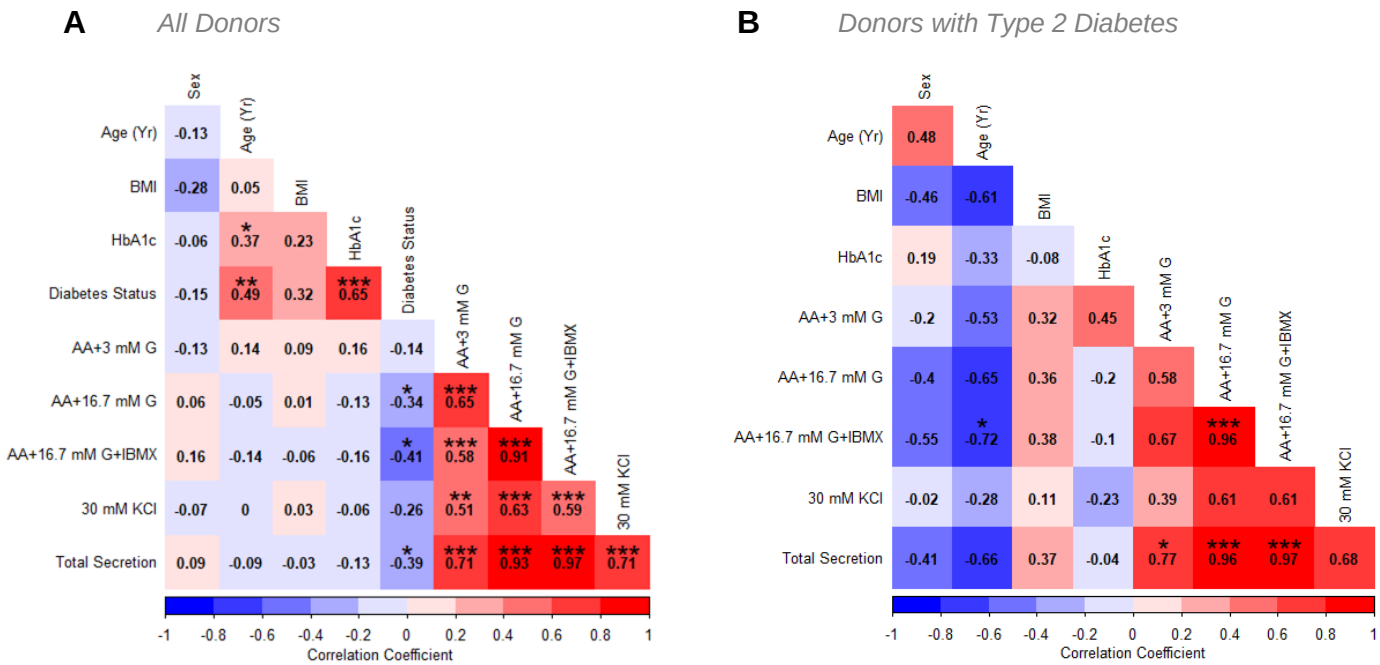
A
All Donors
Sex
Age (Yr)
BMI
HbA1c
Diabetes Status
AA+3 mM G
AA+16.7 mM G
AA+16.7 mM G+IBMX
30 mM KCl
Total Secretion
-0.13
-0.28 0.05
-0.06 * 0.37 0.23
-0.15 ** 0.49 0.32 *** 0.65
-0.13 0.14 0.09 0.16 -0.14
0.06 -0.05 0.01 -0.13 * -0.34 *** 0.65
0.16 -0.14 -0.06 -0.16 * -0.41 *** 0.58 *** 0.91
-0.07 0 0.03 -0.06 -0.26 ** 0.51 *** 0.63 *** 0.59
0.09 -0.09 -0.03 -0.13 * -0.39 *** 0.71 *** 0.93 *** 0.97 *** 0.71
-1 -0.8 -0.6 -0.4 -0.2 0 0.2 0.4 0.6 0.8 1
Correlation Coefficient
B
Donors with Type 2 Diabetes
Sex
Age (Yr)
BMI
HbA1c
AA+3 mM G
AA+16.7 mM G
AA+16.7 mM G+IBMX
30 mM KCl
Total Secretion
0.48
-0.46 -0.61
0.19 -0.33 -0.08
-0.2 -0.53 0.32 0.45
-0.4 -0.65 0.36 -0.2 0.58
-0.55 * -0.72 0.38 -0.1 0.67 *** 0.96
-0.02 -0.28 0.11 -0.23 0.39 0.61 0.61
-0.41 -0.66 0.37 -0.04 * 0.77 *** 0.96 *** 0.97 0.68
-1 -0.8 -0.6 -0.4 -0.2 0 0.2 0.4 0.6 0.8 1
Correlation Coefficient

Figure S3

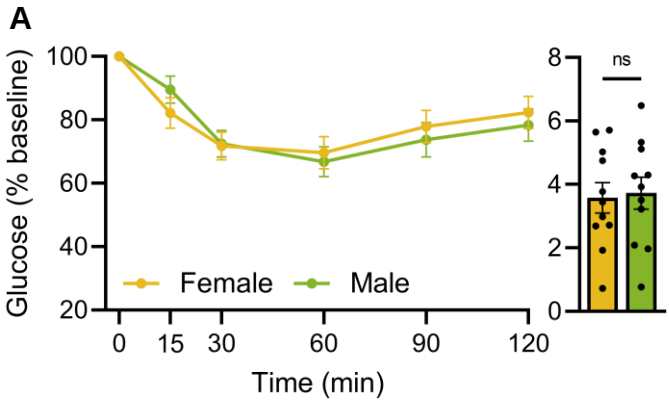
A
Glucose (% baseline)
100
80
60
40
20
0
15
30
60
90
120
Time (min)
Female
Male
8
6
4
2
0
ns

Figure S4

A

Unsupervised Hierarchical Clustering of Mouse Islet Genes
Male 09
Male 07
Male 05
Male 06
Female 07
Female 01
Female 03
Female 06
Female 08
Female 02
Female 04
Female 05
Male 03
Male 04
Male 02
Male 01
Male 08
Column
Z-score
4
2
0
-2
-4

Figure S5

A *Representative Protein Synthesis Staining Images*

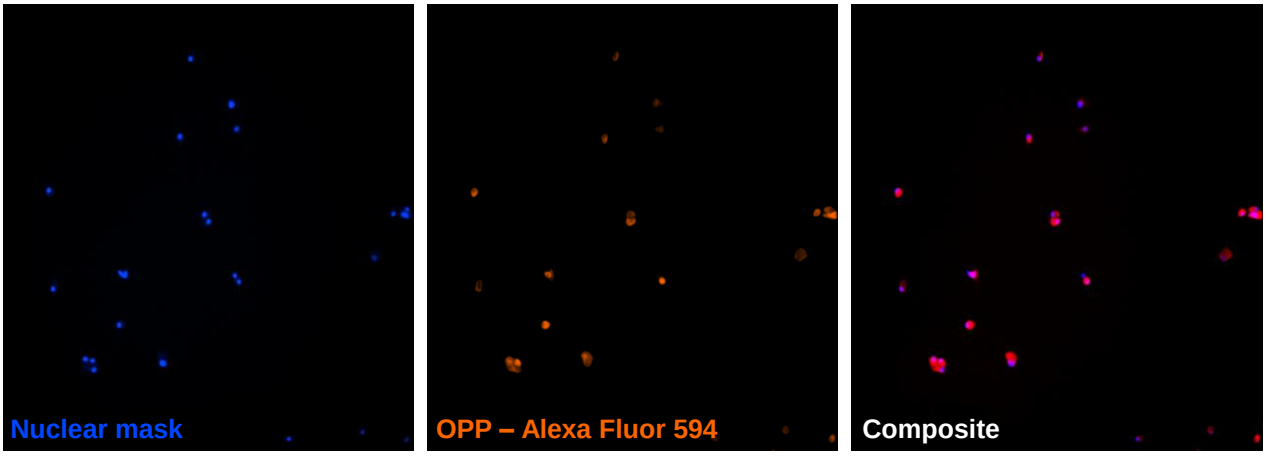

B *Protein Synthesis per Cell*

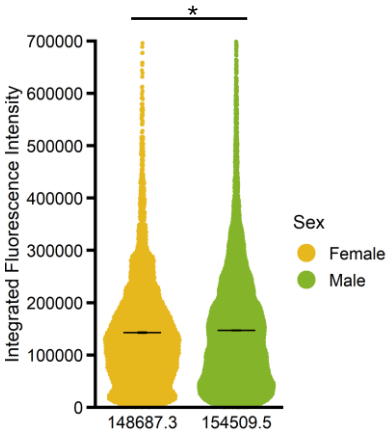

C *Protein Synthesis per Cell*

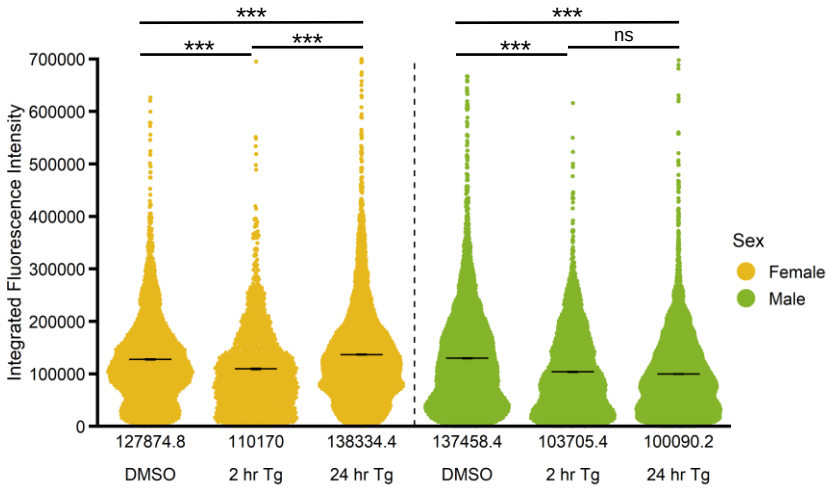

Figure S6

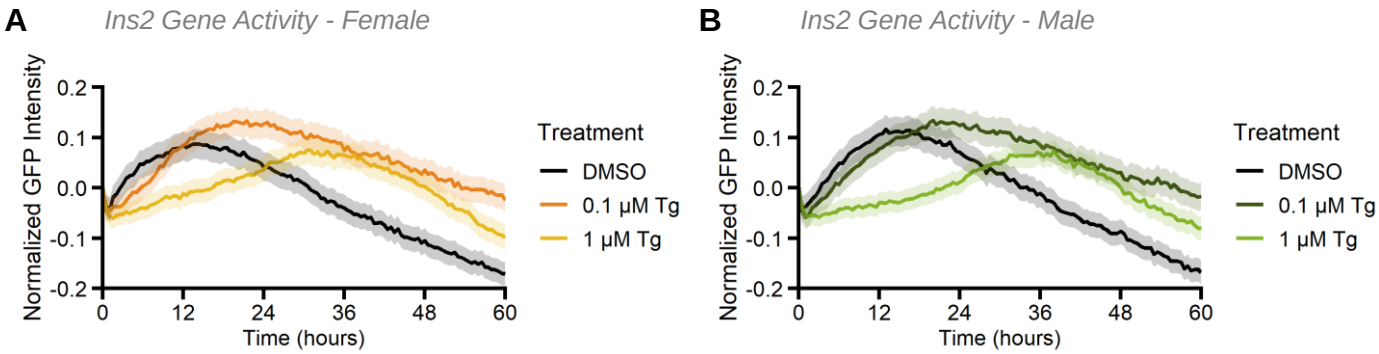
A
Ins2 Gene Activity - Female
Normalized GFP Intensity
0.2
0.1
0.0
-0.1
-0.2
0
12
24
36
48
60
Time (hours)
Treatment
DMSO
0.1 μM Tg
1 μM Tg
B
Ins2 Gene Activity - Male
Normalized GFP Intensity
0.2
0.1
0.0
-0.1
-0.2
0
12
24
36
48
60
Time (hours)
Treatment
DMSO
0.1 μM Tg
1 μM Tg

Figure S7

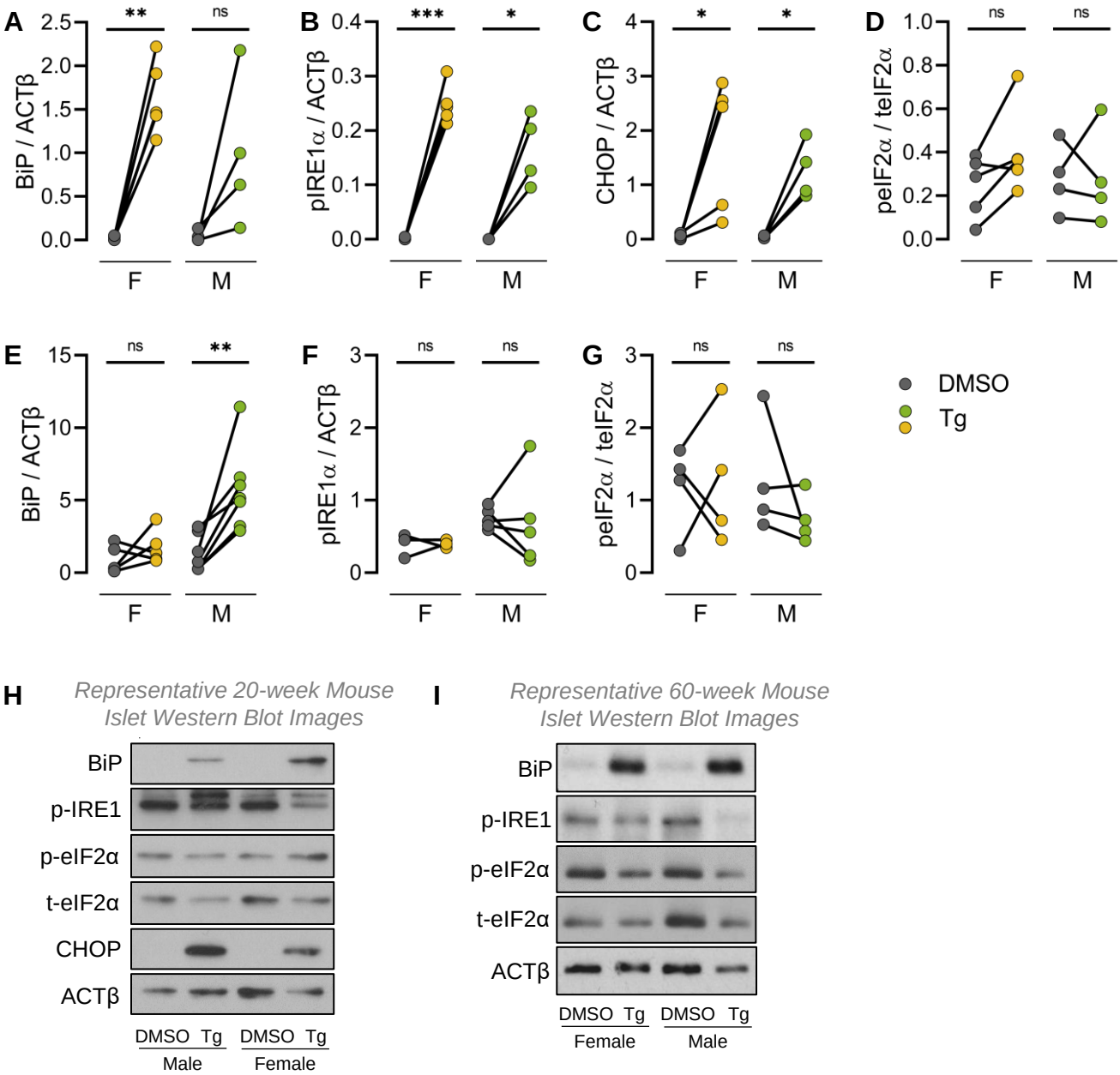
A
BiP / ACTβ
2.5
2.0
1.5
1.0
0.5
0.0
**
ns
F
M
B
pIRE1α / ACTβ
0.4
0.3
0.2
0.1
0.0
***
*
F
M
C
CHOP / ACTβ
4
3
2
1
0
*
*
F
M
D
peIF2α / teIF2α
1.0
0.8
0.6
0.4
0.2
0.0
ns
ns
F
M
E
BiP / ACTβ
15
10
5
0
ns
**
F
M
F
pIRE1α / ACTβ
3
2
1
0
ns
ns
F
M
G
peIF2α / teIF2α
3
2
1
0
ns
ns
F
M
DMSO
Tg
H
Representative 20-week Mouse Islet Western Blot Images
BiP
p-IRE1
p-eIF2α
t-eIF2α
CHOP
ACTβ
DMSO Tg
Male
DMSO Tg
Female
I
Representative 60-week Mouse Islet Western Blot Images
BiP
p-IRE1
p-eIF2α
t-eIF2α
ACTβ
DMSO Tg
Female
DMSO Tg
Male

Figure S8

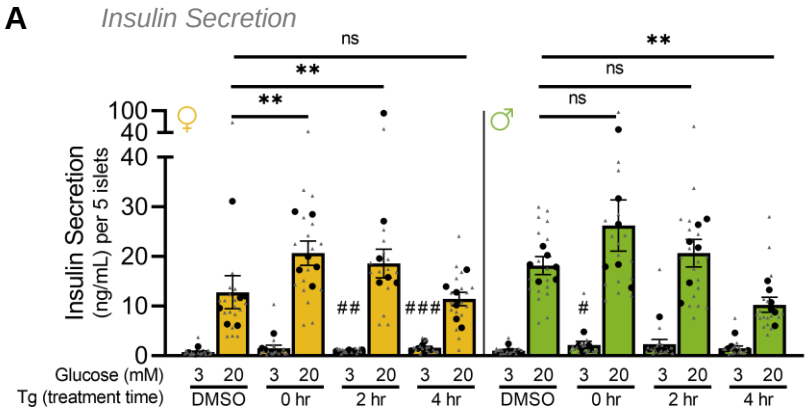
A
Insulin Secretion
ns
**
**
**
ns
ns
100
40
40
30
20
10
0
♀
♂
Insulin Secretion
(ng/mL) per 5 islets
##
###
#
Glucose (mM)
Tg (treatment time)
3 20 3 20 3 20 3 20 3 20 3 20 3 20 3 20
DMSO
0 hr
2 hr
4 hr
DMSO
0 hr
2 hr
4 hr

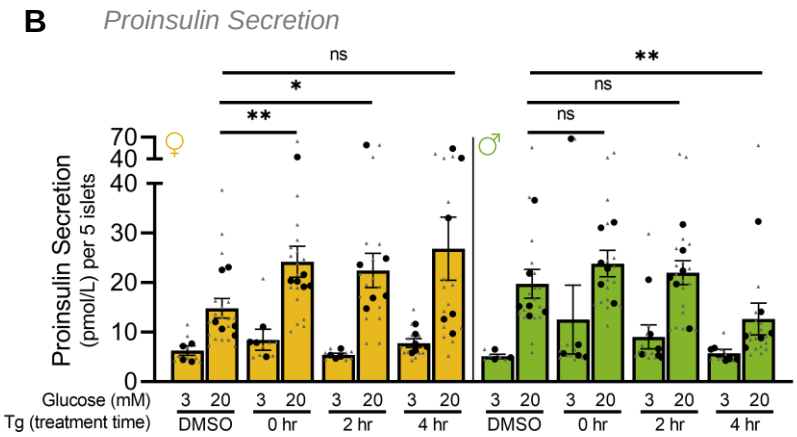
B
Proinsulin Secretion
ns
*
**
**
ns
ns
70
40
40
30
20
10
0
♀
♂
Proinsulin Secretion
(pmol/L) per 5 islets
Glucose (mM)
Tg (treatment time)
3 20 3 20 3 20 3 20 3 20 3 20 3 20 3 20
DMSO
0 hr
2 hr
4 hr
DMSO
0 hr
2 hr
4 hr

Figure S9

A

Unsupervised Hierarchical Clustering of Mouse Islet Genes
Female D 12 hr DMSO
Female A 12 hr DMSO
Male C 12 hr DMSO
Male B 12 hr DMSO
Male A 12 hr DMSO
Male D 6 hr DMSO
Male B 6 hr DMSO
Male A 6 hr DMSO
Male C 6 hr DMSO
Female B 6 hr DMSO
Female C 6 hr DMSO
Female A 6 hr DMSO
Female B 12 hr DMSO
Female D 6 hr DMSO
Male A 12 hr Tg
Male B 12 hr Tg
Male C 12 hr Tg
Female D 12 hr Tg
Female B 12 hr Tg
Female A 12 hr Tg
Male A 6 hr Tg
Male C 6 hr Tg
Male B 6 hr Tg
Female A 6 hr Tg
Female B 6 hr Tg
Female D 6 hr Tg
Female C 6 hr Tg
Column Z-score
4
2
0
-2
-4

Figure S10

A

Islet Pathway Enrichment
[6 hr, DMSO vs Tg]

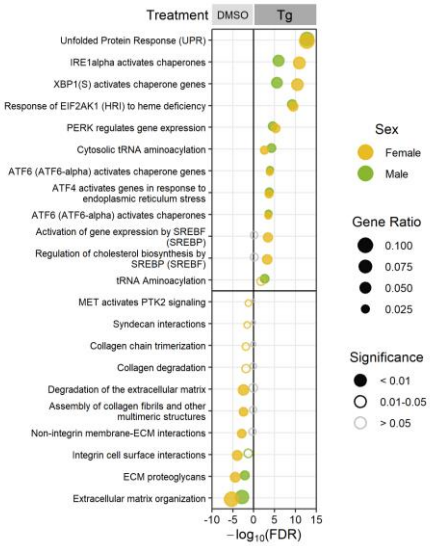

B

Islet Pathway Enrichment
[12 hr, DMSO vs Tg]

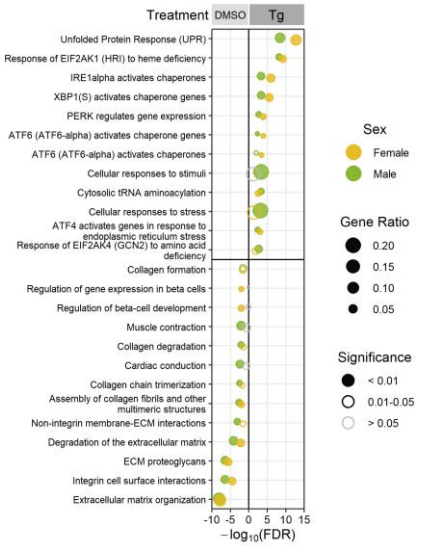

Figure S11

A

β cell identity genes - Female

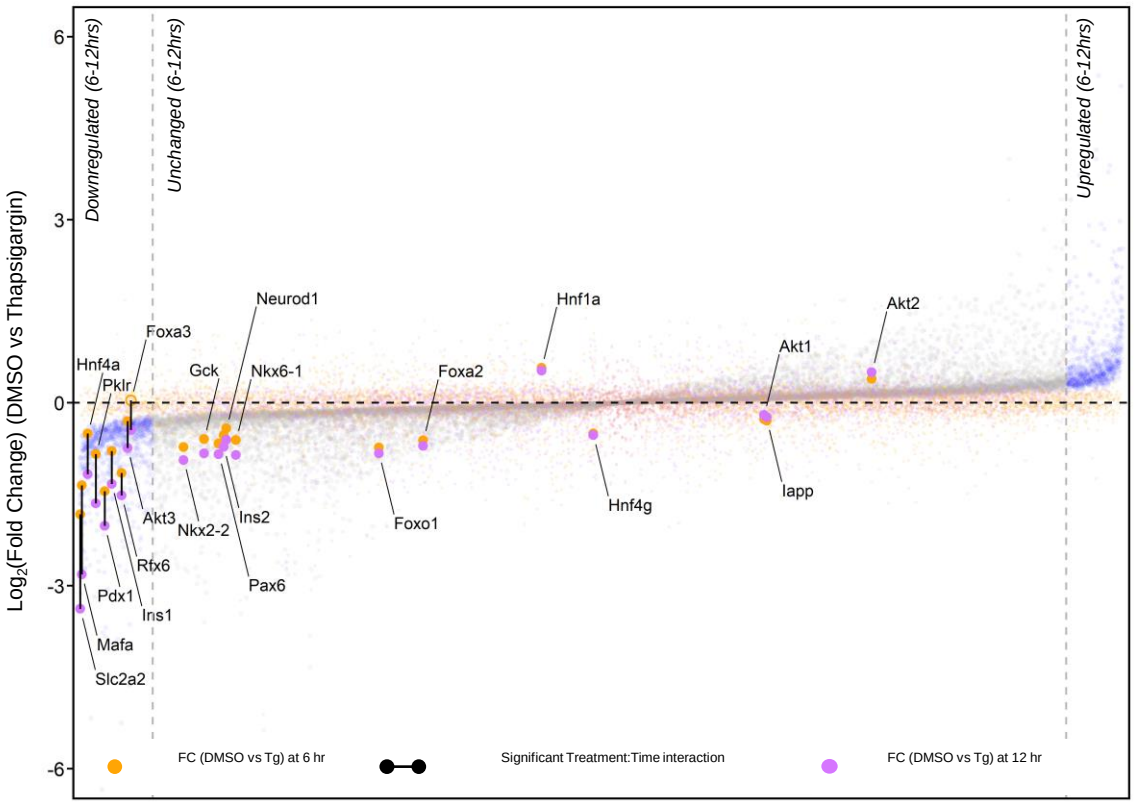

B

β cell identity genes - Male

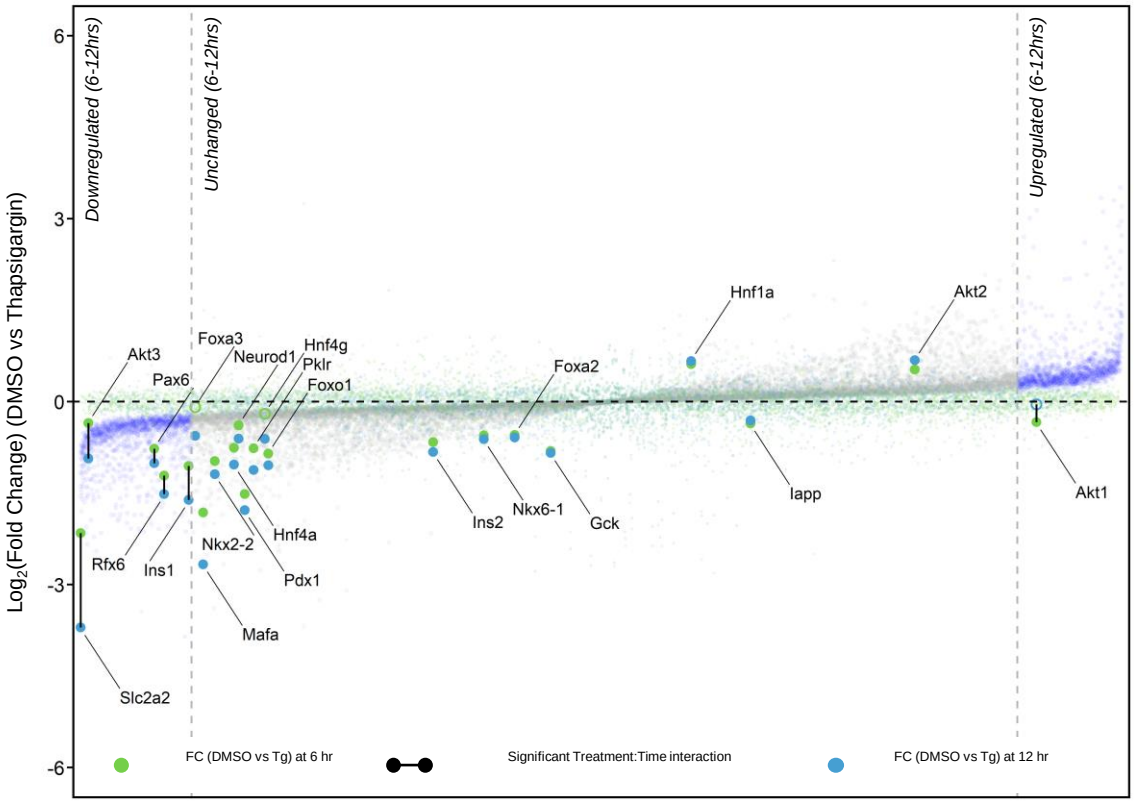

Figure S12